COMPREHENSIVE ANALYSIS AND IMPROVEMENT OF EFFICIENCY, EMISSIONS AND ELECTRICAL POWER QUALITY OF A SMALL, PORTABLE, GASOLINE-FUELED GENERATOR SYSTEM

by

ANDREW GREFF

PAULIUS PUZINAUSKAS, COMMITTEE CHAIR
TIMOTHY HASKEW
MARCUS ASHFORD
JOSHUA BITTLE
HWAN-SIK YOON

A DISSERTATION

Submitted in partial fulfillment of the requirements
for the degree of Doctor of Philosophy
in the Department of Mechanical Engineering
in the Graduate School of
The University of Alabama

TUSCALOOSA, ALABAMA

2019

ABSTRACT

The goal of this dissertation is to explore the methods of improving a small portable gasoline-fueled generator by increasing the efficiency and power quality and also reducing emissions. Advanced engine control strategies and optimized after-treatment systems are employed to achieve the goals. The focus of all three papers is a single-cylinder engine with a low power output which EPA classifies as a non-road spark ignition engine with a power output less than 19 kW. Engines that produce more than 19 kW in the same field can be very similar as they have the same purpose, but have much more stringent emissions standards. Emissions standards drive research and development, so great advances have been made in the higher power engine class, but this development is practically non-existent for low power output engines. Low-power engines are typically single-cylinder which adds additional complexities that must be addressed with unique solutions that higher power, multi-cylinder engines do not experience.

Small portable gasoline-fueled generators use purely mechanical control systems to control all aspects of the engine and have no after-treatment to reduce emissions. Almost every other classification of engine uses sophisticated electronic control systems to control fuel injection, spark ignition, and throttle position to allow for very precise running conditions. Combined with after-treatment systems, these advanced engines produce emissions that are magnitudes lower than the small generator in this study. These low-power engines are used in a multitude of devices such as lawnmowers, handheld garden and lawn equipment, and pressure

washers. There are as many of these devices in the United States as there are vehicles, so by reducing emissions in this class a very large impact can be made.

DEDICATION

This dissertation is dedicated to my Dzia Dzia who started this odyssey of being an engineer for Greffs. Also to my parents who have supported me in every way possible without ever missing a step.

ACKNOWLEDGEMENTS

After what seems like a lifetime, I am beyond pleased to thank everyone that made getting to this point possible. I would like to start with Dr. Paul, my advisor, whom I have now known for 12 years, got me into graduate school, taught me everything about engines, and for some reason kept working with me. I would like to thank Dr. Haskew who showed me a whole new world of controls to expand my passions and would answer every question I had no matter how small or busy he was. The cross-disciplinary knowledge you have helped bestow upon me is beyond invaluable. I would like to thank Dr. Ashford for sharing my passion for racing and being able to talk about anything with me for hours. I cannot thank Dr. Bittle and Dr. Yoon enough for being so cooperative with my difficult schedule and working with me every step of the way. Outside of my committee, there is no one I could ever owe more than Megan Hathcock who for years would sit beside me and then would sit in the lab for hours a day while I was out of state to run my testing for me, generate code, and clean up my spaghetti of code. I would never have finished without you. I would like to thank two of the greatest friends I could have asked for, Chris New and Cole Frederick, for inspiring me every day through our conversations and for stepping up and assisting in testing and setup every time I was drowning. I would like to thank my family for believing in me and always pushing me. Thank you, Sergio, for sitting on a headset with me every day and always finding a way to make me laugh. I would like to thank all of my friends who joked about my graduate date never coming and for always being there for me. Finally, I would like to thank Led Zeppelin, The Who, Foo Fighters, Vivaldi, Miles Davis, and Hans Zimmer for providing an avenue of escape from reality.

CONTENTS

LIST OF TABLES

LIST OF FIGURES

INTRODUCTION

Fixed speed operation is desirable for power generator applications since electrical power output frequency is proportional to the generator rotor rotational speed. Constant electrical power frequency is preferred for inductive loads because it reduces changes in reactive power. Such is true for both large stationary generators as well as small portable units powered by small engines. Small spark-ignited engines are good choices for such portable applications since they are lightweight and inexpensive relative to alternatives such as small diesel engines, gas turbines or fuel cells.

Incorporating advanced technology into small utility engines, such as the control strategies described herein, can potentially significantly improve their efficiency and emission performance compared to baseline low-technology engines. Despite this potential, current EPA emission standards for small engines are very lenient relative to those imposed on larger non-road engines. Table 1 shows the allowable criteria gaseous emissions for both engine categories. Of significant note, small stationary engines have practically no CO restriction compared to their counterparts producing 19 kW or above as mentioned before.

	Nonroad Spark-ignition Engine		
	<19 kW		>=19 kW
Year	2005	2011	2007
HC+NOx	12.1	8	2.7
CO	610	610	4.4
	All units g/kWh		

Table 1. Emission standards for small nonroad engines by year

The lax CO standards are primarily driven by economics. To keep their prices low, these engines are almost all fueled using very basic carburetors that have significant manufacturing variability and limited ability to maintain optimum fuel mixture ratio over broad operating conditions. Furthermore, they are practically all air-cooled to eliminate the cost and complexity of liquid cooling systems. Therefore, they typically are set to take advantage of the lenient standard and operate using air-fuel ratios up to 25% rich of stoichiometric. This is done to improve stability during transient operation, compensate for the aforementioned unit-to-unit variability and control combustion temperature. This lenient standard may give the impression that CO emissions from small engines present no health hazard. Perhaps considering that, at least in the US and other first-world economies, toxic atmospheric CO levels are no longer frequent, this may be true. However, the allowable CO emission disparity coupled with the vast number of small engines implemented in lawn equipment, portable generators and a wide verity of other applications mean the total CO emissions from such engines have the potential to easily surpass those from significantly more tightly regulated mobile sources. Consider that a single 5 kW generator currently emits the same amount of CO as up to 625 idling mid-size late 1990s cars (which certainly do not represent the state of the art in emission control) (EPA, 2017). Figure 1 (CARB, 2017) illustrates that an hour of small engine's run time compares to a passenger car traveling hundreds of miles. Their environmental impact becomes much more significant when considering their ubiquity. The Outdoor Power Equipment Institute reports that 30 million new general purpose engines were manufactured in 2016 with an estimated 100 million owned in the country (OPEI, 2017). Considering this number is essentially equivalent to the approximately 100 million registered cars in the US, it would seem there should be ample motivation to reduce their impact on atmospheric air quality.

A much more severe concern is the danger these engines pose when operating in close quarters at their allowable CO limit. Between 2004 and 2012, 659 fatalities were caused by the use of general purpose engines due to CO poisoning. Ninety-four percent of those occurred from operating the engines in an enclosed space, but the remaining six percent occurred even with the engine located outdoors. This happens when low velocity wind blows the high concentration engine emissions into houses with minimal mixing and dispersion. This is most common during storm-caused power outages where consumers are tempted to run portable generators near open windows or in open garages if it is still raining. Exposure to CO levels over 70 ppm for extended periods of time are considered hazardous. Exposure at levels of 150 to 200 ppm and above can cause permanent brain damage or death (CPSC, 2006).

Previous work supported by the US Consumer Product Safety Commission (CPSC) and performed at The University of Alabama to develop a low CO-emission portable generator prototype demonstrated a 93% CO emission level reduction is possible using conventional engine control and exhaust aftertreatment systems (Buyer, 2012). An extension of this effort also included the development of passive methods integrated into the engine control system to detect high ambient CO levels and subsequently shut the engine off under these circumstances (Haskew & Puzinauskas, 2013). The CPSC movement to reduce emissions is likely to be resisted due to cost, so being able to minimize the amount of expensive catalyst mass would help to achieve future goals. The original Buyer (2012) report provides data indicating that near stoichiometric operation of a small, air-cooled utility engine is possible without substantial degradation to longevity, thereby indicating an opportunity for considerable emission reduction through improved fuel control even without the catalyst.

Figure 1. Equivalent emissions for small engines (CARB, 2017)

Dissertation Overview

This dissertation consists of three standalone papers that each focus on improving portable generator performance through improved control and application of emission aftertreatment to the engine. The first investigates the benefits of applying modern electronic engine control to small, general purpose applications. That paper furthermore explores the implementation of an anticipatory control strategy facilitated by the associated electronic control hardware. The second paper identifies the challenges associated with implementing exhaust aftertreatment on a small single cylinder engine and compares the performance achieved for given catalyst sizing in single cylinder versus multi-cylinder applications. The third paper investigates the impact the improved electronic control has on the electric power quality delivered in a portable generator application.

The following sections consolidate the technical background from each of these papers and enable the reader to focus on the unique specifics and results of the papers that follow. The first section will be about the engine controls necessary to run advanced algorithms on the

engine, then catalyst construction and methodology will be discussed, and finally, the alternator will be described.

Engine controls

Traditional (low-technology level) small engines use entirely mechanically based systems for controlling speed, fuel, and spark. Many designs are simplified carryovers from vehicle systems from decades or even a century ago. Without the stringent emissions requirements like vehicles face, the small engines have been able to survive with the mechanical solutions not requiring any further research or design. The following paragraphs discuss traditional engine speed, fuel and spark control that are typical of current small engines on the market in order to provide context to the description that follows of electronic systems that control these parameters.

Mechanical Speed Control. The traditional method of controlling speed is through a mechanical governor such as the centrifugal flyball governor shown in Figure 2. This device is based on the kinetic energy of weights spinning with a rotational velocity proportional to the engine's crankshaft. A linkage mechanism connects these weights to the engine's throttle. As their rotation speed increases, the weights move outward causing the throttle to close. This arrangement provides proportional engine speed control by balancing the torque produced by the engine with the applied load to the engine. Such a proportional system suffers from inherent speed droop with load. This is because more airflow is required in the engine to increase torque, and to provide the extra air needed to produce the torque, the throttle has to open more which only happens with reduced speed. Increasing the proportional gain (the lever ratio between the balls and the throttle or reducing the spring stiffness (when present) that restrains the flyballs will reduce the droop but will increase the tendency for the speed to overshoot its setpoint. To

eliminate the droop and control the overshoot, integral and derivative effects must be incorporated into the mechanism.

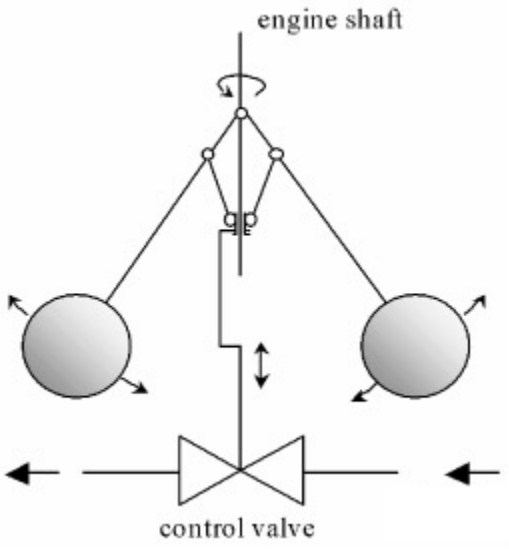

Figure 2. Control schematic for centrifugal governor (Spec, 2006)

Mechanical solutions for the integral and even derivative terms have been designed, but are incredibly complicated and expensive. Figure 3 gives an example of a system that controls proportional, integral and derivative terms and shows the complex mechanical systems it requires.

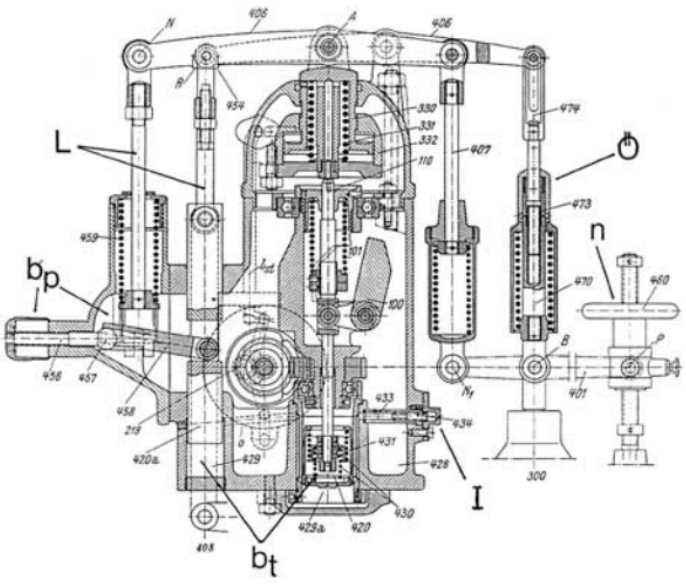

Figure 3. Mechanical governor with proportional, integral, and derivative capabilities (Springer, 1940)

Mechanical Fuel Control. Traditional fuel systems use a carburetor to control the proportion and amount of fuel and air delivered to the engine. Most carburetors primary fuel proportioning occurs using the pressure drop created by passing the entering air through a venturi. A wide variety of auxiliary mechanisms have been developed and implemented on various designs to augment this base fueling rate in order to compensate for transient conditions, high and low load operation as well as cold start. The OEM carburetor which the engine in this study came equipped with was a diaphragm type which is designed for ease of manufacturing and low price. The diaphragm design precludes more sophisticated mechanisms designed to improve fuel control over the engines steady state operating range. It also cannot provide acceleration enrichment either because the metering chamber is sealed from the atmosphere and keeps a vacuum to operate the diaphragm and fuel needle (Woody, 1975). These design choices lead to high fueling error and poor atomization which require overly rich calibration to insure fueling levels never fall below minimum requirements for combustion stability and engine

cooling under all operating conditions. This rich operation leads to high carbon monoxide and hydrocarbon rates as discussed in the motivation section above.

Mechanical Spark Control. Small engines have almost exclusively used a magneto ignition system. While such a system is strictly speaking an electro-mechanical system, the moment when the spark is induced is completely mechanically controlled. The induced spark is created by a magnet installed at a specific location on the engine flywheel (note, this is not the flyweights that are used in the mechanical governor described above). This magnet then passes under a coil which is fixed to the engine case, and the moving magnetic field energizes the coil. Once the magnet passes, the field collapses and is converted into a high voltage that delivered to the center electrode of the spark plug. If the voltage is high enough to jump the gap from the center electrode to the ground strap, a spark is created that initiates combustion of the fuel-air charge trapped in the combustion chamber. This system sparks every revolution of the engine and at effectively the same crankshaft angle every time.

All of the aforementioned mechanical control systems are proven and robust technologies. They don't require any computerization which allows them to be manufactured very cheaply, resist failures, and be easily serviceable if they do need any repair. However, the limited ability to optimize these systems under broad operating conditions prevents significant progress in emission reduction and efficiency improvements. Carburetor-based fuel control system limitations, in particular, could not meet any further reduction in future emission regulations, especially as the engine ages. The fixed magneto ignition system has no spark timing control at all. Consequently the fixed spark angle is chosen as a compromise for all conditions which often leads to poor combustion phasing at various loads. Finally, the speed control is inherently error-prone as the engine cannot exceed its maximum speed, but must inherently decrease in speed at

load due to its design. Furthermore, the system is also entirely reactive instead of being proactive which amplifies the carburetor's fuel control errors during load changes.

Electronic Engine Control Overview. In contrast to these mechanical counterparts, electronic fuel, spark, and actuator control allow for flexible calibration at all speeds and loads. The fuel delivery quantity and timing is precisely matched with airflow that is either directly measured or calculated from related parameters in order to optimize the fuel-to-air proportion and charge preparation based on operating conditions. The spark phasing can also be easily calibrated to vary through the speed/load range to maximize torque and combustion efficiency. Integral and differential terms can easily be added to electronically controlled and actuated throttles thereby eliminating the inherent droop and substantially improving the response and stability of purely proportional control. All these improvements require additional sensors to measure the relevant parameters and actuators to adjust the controlled variables; however, advances in design and mass production techniques have brought high volume prices of such devices literally to pennies in some circumstances. Electronic systems can also be enhanced with feedback signals to verify if control commands are producing the desired outputs and adjust them accordingly if they are not. These are particularly useful for the fuel and throttle control systems.

The first electronic systems were implementation independently. Electronic ignition systems were incorporated in automotive applications before electronic fuel control systems. Electronic throttle control was first implemented in stationary applications requiring governed speed control such as generators or industrial equipment and was often implemented without electronic ignition or fuel control. Modern systems, however, are fully integrated with either a central computer controller or distributed controllers that communicate with each other. Such coordinated control systems provide extensive opportunities to optimize engine performance. In

particular, and the subject to this effort combined electronic throttle and fuel control implies the control algorithm has a priori knowledge of both the fuel and air flow future and can use that information to prevent over or under fueling during operational transients. In stoichiometric strategies, over fueling will create excess HC and CO emissions while under fueling will create NOx. Minimizing these excursions would be an effective method of reducing emissions.

Fuel control algorithms have been developed to reduce emissions during such rapid load changes, but they have been for multi-cylinder air control. One solution is to use a differential mass flow equation for the intake manifold (Piero Azzoni, 1999) which predicts the airflow change that occurs with changed throttle angle. The differential equation is with respect to crank angle in their research. The change in flow can then be integrated over the entire cycle to determine the total mass ingested by the cylinder. Due to it being a multi-cylinder engine, they are able to determine the throttle change through the rate of pressure change instead of directly monitoring the throttle angle. Single cylinder engines do not have intake manifolds though, and under high load conditions, their entire intake system empties and fills itself multiple times per engine cycle. Mass flow for a single-cylinder engine can be predicted in computer analysis, but it is very complicated and computational intensive (Shun-ichi Akama, 2013). Such a model must be integrated with at least crank angle degree to accurately represent the physics.

Very few OEM electronic control applications have been developed for the small utility engine market sector because of the lenient emissions requirements; however, such technology becomes common as soon as the output crosses the 19 kW threshold. These control systems are expensive relative to the cost of small engines, sometimes almost as much as the engine costs itself. They also require much more development time for calibration than mechanical systems; and this calibration, as described below, presents particular challenges due to the flow dynamics

associated with single-cylinder engines. However, the improved fuel and spark control enable higher combustion efficiencies and increased torque and also lead to a substantial reduction in emissions. Furthermore, the previously cited report by Buyer (2012) indicates that the fuel savings associated with a stoichiometric fuel control strategy will more than pay for this economic cost over the life of the engine.

There are multiple companies that offer aftermarket solutions for small engines, but those are generally for motorsports purposes. The only engines under 19 kW with electronic controls made for non-road purposes is made by Kohler. Their most general-purpose engine is the Command Pro EFI ECH440 which is a 429 cc engine that outputs 10.4 kW (Kohler, 2019). It is used in equipment such as air compressors, blowers, and generators.

The next paragraphs give additional details regarding electronic throttle and fuel control systems given their central role in the present work

Electronic throttle control. Electronic throttle control has fundamentally changed how airflow is used to set an engine's operating condition. Whereas traditionally mechanical systems link to a speed control governor as described above or to a mechanism such as a gas-pedal when direct operator control is desired, modern systems simply monitor the associated outputs of those devices as one of many inputs used to determine the best throttle position. Current automotive systems, for example, use an air-based control strategy with the accelerator pedal position as one of its inputs (Prince, 1998). This strategy assumes pedal is correlated to power and then moves the throttle to match the airflow required preemptively instead of reacting to changing conditions in a reactive system. This helps reduce fueling error and can also provide many other benefits such as torque control and catalyst oxygen storage control. The torque control allows for the engine controller to work more smoothly with transmission controllers during shifts by

determining how much torque must be reduced to provide a smooth shift (Ganoung, 1990). Throttle control on modern systems is very complex due to engine being non-linear. To build a model, engines must be run at thousands of points with various conditions to study the impact of airflow, fuel injection timing, and spark timing. It takes weeks or months to run and analyze, and the model is the top consumer of processing power for the engine controller.

Electronic Fuel Control. Electronic fuel control systems consist of three main components or subsystems that perform the following tasks: 1) Air flow measurement, 2) Fuel delivery, and 3) fuel-air ratio feedback. Air flow is measured using one or more of three standard methods to calculate airflow. The first method, alpha-N, uses throttle angle and engine speed as independent variables to a calibrated airflow lookup table. Its accuracy depends entirely on the calibration and does not adapt to system changes since it relies on that table without any corrections. The next method is speed-density which is based on a similarly calibrated volumetric efficiency table; however, measured manifold air pressure and temperature are used to calculate the density term in the volumetric efficiency definition that yields airflow.

Consequently, the airflow calculation incorporates the operating conditions more directly than the Alpha-n method and makes it more robust. Speed-density is the method used in this work, so specific details on how it is implemented are provided in the following papers. The last method is a direct measurement of air flow using a hot-wire anemometer and is the most accurate of the three methods. A production automotive airflow sensor cannot respond to rapid changes in air velocity though due to design, so it is only used at steady-state points.

While the latter two methods are considerably more accurate in multi-cylinder engines, there are significant challenges to implement them in one or two cylinder engines. The application is simplified in multi-cylinder engine because there is generally always at least one cylinder

drawing air in from the intake system and the airflow and conditions in the intake manifold are relatively steady. In contrast, the extreme intake and exhaust velocity and pressure fluctuations associated with single-cylinder flow dynamics render the mass airflow meter unusable since the air is moving continuously in alternating directions in the intake port. These pulsations also add a level of complexity to the speed-density method because the pressure downstream of the throttle changes throughout the cycle and the dynamics are different depending on throttle angle. At low load with the throttle nearly closed, the pressure approaches atmospheric during the intake-valve closed portion of the cycle, then drops dramatically during the intake stroke. The associated pressure excursion dampens out rapidly at the throttle. At high load with the throttle near wide open, the pressure excursion alternates as a pressure pulse as it oscillates up and down the runner. This makes it critical to measure the pressure at a very specific point in the cycle to infer load from that measurement. The minimum pressure during the intake stroke gives the best indication of load. Because the point in the cycle at which this occurs varies with speed and load itself, another speed and load dependent table must be calibrated to specify the crank angle at which to make the measurement. This crank angle is known as the 'MAP read angle.' Calibrating this table can be complicated when the manifold pressure sensor is remote mounted and communicates with the measurement runner location with a tube. This has the side effect that fueling is always a cycle behind since the MAP measurement is taken during the intake stroke of the previous cycle.

Fuel Injection. Low-cost systems use a port fuel injector in the engine head pointed at the intake valve. For low emission applications, the injection is timed to occur while the intake valve is closed to allow the heat of the valve to evaporate the fuel into a gaseous mixture which will burn more efficiently. To maintain this timing in multi-cylinder engines, the injectors must be

able to be independently controlled, which is known as sequential port fuel injection. This is not an issue in a single-cylinder engine. Even with appropriate timing, liquid fuel still accumulates on the port walls, which is a significant issue since the amount accumulated varies with load. This means that all the fuel injected for the current cycle may not make it into the cylinder, or conversely, fuel in addition to that injected may enter. Models have been developed to account for this fuel film (Cheng, 2000) to help during transient events as manifold pressure changes. As the pressure changes, the vaporization temperature of the fuel changes leading to the film changing thickness. This can lead to either fuel being deposited or removed from the film and becoming unaccounted for in the fueling control. Injecting while the valve is closed helps to prevent the need to calibrate the complex film model, and it may also be debatable of its usefulness in a single-cylinder engine that varies manifold pressure considerably every cycle.

Electronically controlled fuel delivery is usually monitored using a universal exhaust gas oxygen (UEGO) sensor to infer fuel-air ratio. This sensor is used for feedback control strategies which continuously modify the calculated injected fuel mass to account for conditions unaccounted for in calibration as well as for both short and long-term learning which can compensate for component wear.

Catalytic Converters

Engine exhaust emissions reduction efforts typically combine some combination of two strategies. First, the emissions leaving the exhaust port can be reduced through the development of the combustion system and second, these engine-out emissions can be further reduced using an exhaust after-treatment system. Most after-treatment systems incorporate some type of catalytic converter which facilitates chemical reactions which convert the harmful emissions to less toxic or benign species. The following paragraphs describe the global strategy of the two

most common automotive catalyst types used in spark-ignition engines. These descriptions are followed by an overview of the materials and structure that facilitates these strategies.

There are two main types of catalytic converters used on spark-ignited engines. The first automotive application used the two-way catalytic converter, which was introduced in 1975 to meet the increasingly restrictive emissions standards in the US. The 'two-way' designation stems from its function to remove two criteria emission species from the exhaust- carbon monoxide (CO) and unburned hydrocarbons (UHC). To convert them into less toxic gases, both gases are oxidized using surplus air in the exhaust. In the original applications, the engine would operate in a fuel-rich condition to prevent NOx formation and a crankshaft driven air pump would be used to add air into the exhaust which would be able to oxidize the CO and UHC at the low exhaust temperatures in the presence of the catalyst. This strategy would not be used in modern automotive applications due to the decreased efficiency associates with rich operation and the parasitic loss of the air pump. Two-way catalysts are used today in lean burn applications, however, since by definition the charge inherently contains more than enough air needed to completely oxidize the fuel- preferably in the combustion chamber or in the exhaust aftertreatment system if necessary. In such operation, the charge is either kept lean enough such that combustion temperatures remain too low for significant NOx production or the two-way catalyst is combined with an additional NOx trap to catalyze the NOx (Farrauto, 2002). The global oxidation reactions in a two-way catalytic converter are:

$$2CO + O_2 \rightarrow 2CO_2 \quad (1)$$

$$CH + O_2 \rightarrow CO_2 + H_2O \quad (2)$$

The three-way catalyst was developed a few years later to reduce the efficiency impact associated with two-way air-pump implementations and to meet the US EPA's reduction in

allowable NOx emissions from light-duty vehicles that were to be enforced beginning in 1981 (EPA, 2016). As might be deduced, 'three-way' refers to adding NOx reduction to the original CO and HC oxidation of the original two-way catalyst. This additional function significantly increased the complexity of the catalyst design and implementation since oxidation is favored under lean conditions while reduction occurs under rich conditions. Consequently, the engine must operate around stoichiometric fuel-air proportion with carefully controlled rich and lean excursions. It must do this to build reserves for each reaction, as emissions typical when rich (CO and HC) need the emissions that are typical for lean (NO) to react and vice versa. To be effective, the switching frequency around stoichiometric should be around .5 to 1 Hz and fueling deviations as much as 1 AFR can be tolerated in each direction as long as this switching is maintained (Heywood, 1988). In addition to the two-way oxidation reactions shown above, the three-way catalyst adds three NO reduction reactions, which use stored CO, UHC, and hydrogen, respectively:

$$2CO + 2NO \rightarrow 2CO_2 + N_2 \quad (3)$$

$$CH + NO \rightarrow CO_2 + H_2O + N_2 \quad (4)$$

$$2H_2 + 2NO \rightarrow 2H_2O + N_2 \quad (5)$$

Materials. The first component of a catalytic converter is the substrate, which acts as the backbone which the catalyst materials are placed upon. It must be an inert material that can withstand the extreme environment it works in. Ceramic is generally chosen due to its ability to function in high temperatures and its ability to be easily extruded into many shapes. A honeycomb design is used due to its high surface area per unit volume taken up in the airflow. The airflow must be as unimpeded as practical to prevent additional backpressure on the engine

but must have enough surface area to successfully treat the emissions. In extreme temperature situations, metal substrates are used with the negative of a high manufacturing cost.

The washcoat is the second component of a catalytic converter. It is another inert material that the catalyst is suspended within. Its purpose is to provide a method to apply the catalyst to the substrate with the maximum surface area possible. To do this, it creates a very porous finish. Materials typically used as the washcoat include aluminum oxide, titanium dioxide, silicon dioxide, or a mixture of silica and alumina.

The catalysts come in the form of three rare metals: platinum, palladium, and rhodium. These are very expensive and rare metals so designers must optimize every aspect of the catalyst design to reduce the mass required. Platinum is generally the most common material used as it can both oxidize and reduce the emissions. Palladium can only oxidize, and rhodium can only reduce, so the two are generally used in tandem.

To effectively process the emissions, a steady flow of exhaust gas is needed to build reserves of the necessary constituents for each reaction. Multi-cylinder engines are very helpful in this aspect because they effectively are continually flowing from the effect of at least one cylinder blowing down exhaust throughout the engines revolution. A single-cylinder engine adds complexity though with flow occurring both directions since the exhaust pulse only lasts for about 25% of the time. This leads to stagnant emissions, processed emissions, and possibly fresh oxygen from after the exhaust pipe flowing over the catalyst multiple times per cycle which requires a larger mass of catalyst to be able to cope with the additional residence time.

Alternator

An AC synchronous generator, or alternator, is one in which the frequency of the output voltage and current is directly proportional to the rotor speed. The generator has windings on

both the rotor and the stator. To establish the magnetic field in the air-gap of the generator, a winding on the rotor is excited with a DC current. The resulting rotating magnetic field induces a sinusoidal voltage on the stator winding which supplies the power to meet the load. The DC rotor current controls the magnitude of the voltage induced on the stator. A simple voltage regulator on the rotor winding provides a cheap and robust solution to control rotor current, and hence output voltage.

The power output of the genset is proportional to the square of the magnetic flux produced on the rotor. The current that controls the rotor magnetic flux is determined by the onboard voltage regulator. The voltage regulator taps the outputs of the stator to measure the voltage output, rectifies the ac signal, and then scales the current necessary to achieve the desired output voltage. An example of a voltage regulator control scheme is shown in Figure 4.

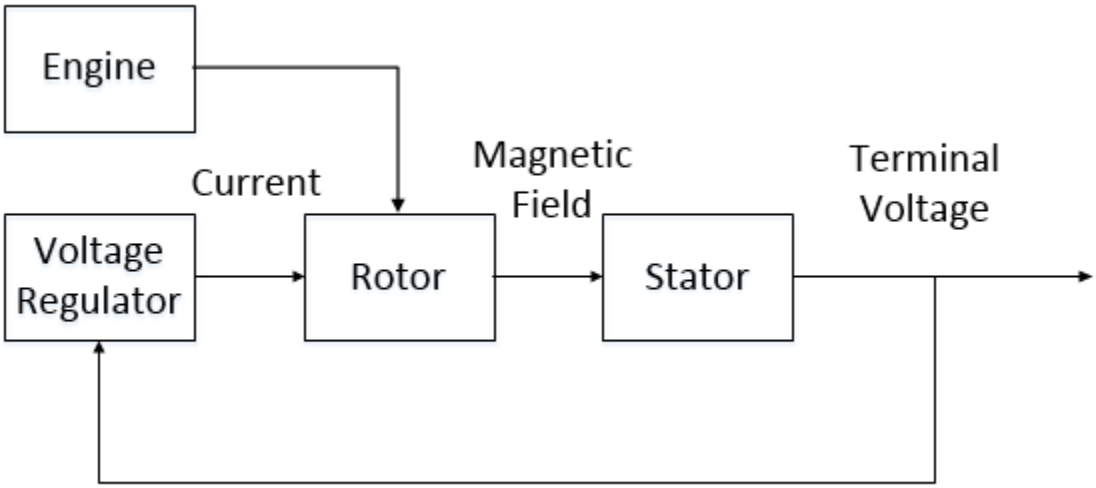

Figure 4. Simplified diagram for method of controlling voltage output of generator

As the load increases, the terminal voltage will sag due to the winding impedance. The voltage regulator will then increase the current on the rotor to boost the voltage back up to operating range. Another condition is as the frequency droops, the generator's reactive power

output increases, and the voltage regulator must also boost its current to make up for the resulting real power losses that occur with the increase in load current.

The voltage regulator does not affect the output frequency, so the frequency of the genset is directly defined by the engine speed. This means the output frequency droops under heavy loads if proportional only engine speed governors are used such as the mechanical fly ball systems previously described. More expensive generators will use multiple stators to allow for voltage control and also for reactive power reduction (Saptarshi Basak, 2017), but this is too expensive of a solution for low power applications.

Most generators available for home use in the United States are designed to run at 3600 RPM to provide the 60 Hz frequency used for all AC powered devices. In power plants, very complicated and important control systems are in place to minimize any frequency disturbance and to keep the long-term average at a very precise 60 Hz. The power-grid system frequency control is also helped by having many interconnected synchronous generators that all are spinning at the same speed and resist any change (Mobarak, 2015). Some systems limit load to maintain a maximum rate-of-change on certain parameters to keep them within limits (Cruden, 2007). Although power plants are very resilient to load changes, even commercial power solutions such as wind turbines can experience power factors as low as 0.5 during a load change (Md Moinul Islam, 2016).

Portable generators currently force consumers to accept the penalties for frequency deviation and hope no harm is done to the devices the generator's power. This allows for cheap engines to be used to power the generator and have a wide speed range. Generators are generally set to run at 3600 RPM at no load which means that engine speed will only become lower as load is applied, so the max frequency seen by any load will be 60 Hz.

Figure 5 shows the equivalent circuit for a typical generator. It has been simplified to contain a resistance (R_s) and reactance (X_s), which is equal to the product of frequency and impedance, to characterize the generator. The terminal voltage (V_t) represents the interface to the user loads, and the load is simply a resistance (R_L).

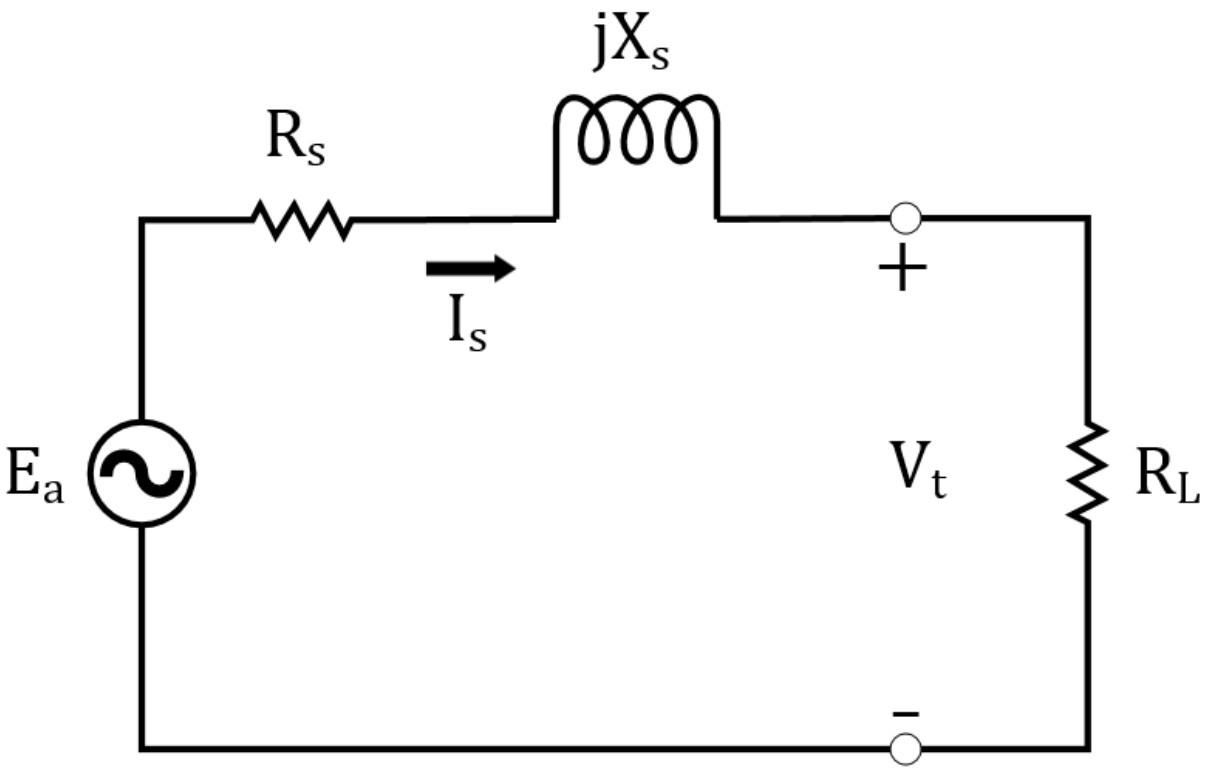

Figure 5. Schematic of generator with resistance load

The frequency deviation has an effect of the apparent power produced by the generator. For a given load, the resistance and inductance will remain constant. Equation 6 shows how current for the system is calculated.

$$\bar{I}_s = \frac{V_t}{R_L + j\omega L_L} \tag{6}$$

Since voltage will remain controlled by the voltage regulator, and the resistance and inductance will both remain constant, the system current will increase due to the reactance from the inductive load decreasing. The increased current leads to higher losses due to heat generation in the windings from resistance as noted in Equation 7.

$$P_{loss} = \bar{I}_s^2 * R_s \tag{7}$$

The heat loss decreases the efficiency of the generator and proportionally increases the fuel required to produce a given generator load. The reactance also creates an undesirable type of power called reactive power which cannot be used by the load. By plotting complex power in the complex plane (Figure 6) where real power (P) is on the real axis, and reactive power (Q) is on the imaginary axis, the magnitude becomes known as apparent power (S).

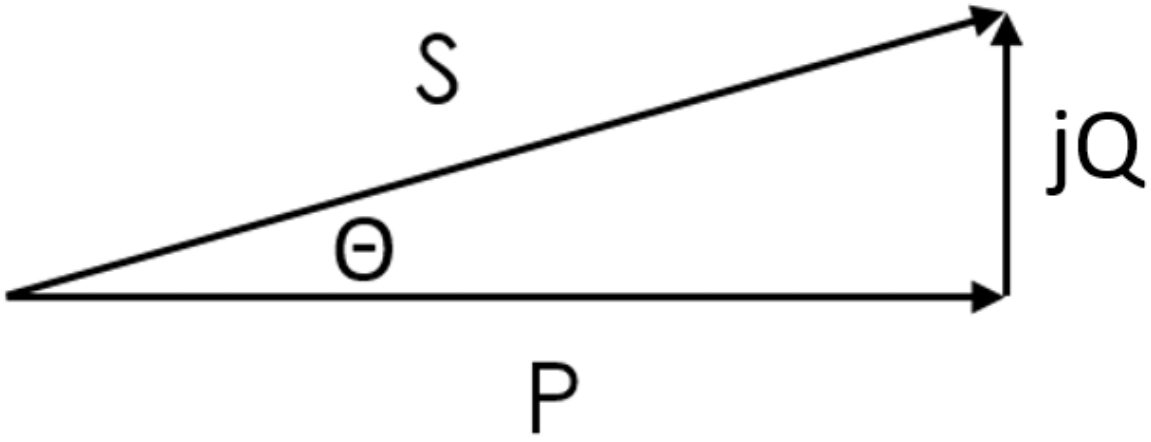

Figure 6. Power phasor diagram

So as reactive power increases, apparent power must also inherently increase. This increase in apparent power, especially at reduced power factors, leads to less real power being able to be delivered at peak load for a given diameter of the motor winding wire. This is due to the apparent power increasing the current of the system and requiring additional wire diameter to

flow. The engine operating at 60 Hz will reduce the reactive power at a given load and improve the efficiency of the overall system.

DEVELOPMENT OF A PREDICTIVE AIRFLOW ALGORITHM BASED ON EMPIRICAL FLOW DATA TO REDUCE HYDROCARBON EMISSIONS

Introduction

General purpose utility engines are designed for a wide variety of applications. They range in power up to 19 kW, are intended for non-road use only, and usually operate over a narrow speed range with varying loads. This works well for applications such as power generators, lawn mowers, or handheld lawn equipment.

Fixed speed operation is desirable for power generator applications since electrical power output frequency is proportional to the generator rotor rotational speed. Constant electrical power frequency is preferred for inductive loads because it reduces changes in reactive power. Such is true for both large stationary generators as well as small portable units powered by small engines. Small spark-ignited engines are good choices for such portable applications since they are lightweight and inexpensive relative to alternatives such as small diesel engines, gas turbines or fuel cells.

This paper describes work performed to develop and implement a predictive fuel control algorithm on a small utility engine in order to improve fuel-air ratio control during engine transients and consequently lower emission during transient operation. The remainder of this introduction provides the motivation for this work, some basic background on engine control and finally states the objective of this work.

Motivation

Incorporating advanced technology into small utility engines, such as the control strategies described herein, can potentially significantly improve their efficiency and emission performance compared to baseline low-technology engines. Despite this potential, current EPA emission standards for small engines are very lenient relative to those imposed on larger non-road engines. The EPA uses a 19 kilowatt power output threshold to distinguish non-road spark-ignition engines. Table 1 shows the allowable criteria gaseous emissions for both engine categories. Of significant note, small stationary engines have practically no CO restriction compared to their counterparts producing 19 kW or above.

	Nonroad Spark-ignition Engine		
	<19 kW		>=19 kW
Year	2005	2011	2007
HC+NOx	12.1	8	2.7
CO	610	610	4.4
	All units g/kWh		

Table 2. Emission standards for small nonroad engines by year

The lax CO standards are primarily driven by economics. To keep their prices low, these engines are almost all fueled using very basic carburetors that have significant manufacturing variability and limited ability to maintain optimum fuel mixture ratio over broad operating conditions. Furthermore, they are practically all air-cooled to eliminate the cost and complexity of liquid cooling systems. Therefore, they typically are set to take advantage of the lenient standard and operate using air-fuel ratios up to 25% rich of stoichiometric. This is done to improve stability during transient operation, compensate for the aforementioned unit-to-unit variability and control combustion temperature. This lenient standard may give the impression that CO emissions from small engines present no health hazard. Perhaps considering that, at least

in the US and other first-world economies, toxic atmospheric CO levels are no longer frequent, this may be true. However, the allowable CO emission disparity coupled with the vast number of small engines implemented in lawn equipment, portable generators and a wide verity of other applications mean the total CO emissions from such engines have the potential to easily surpass those from significantly more tightly regulated mobile sources. Consider that a single 5 kW generator currently emits the same amount of CO as up to 625 idling mid-size late 1990s cars (which certainly do not represent the state of the art in emission control) (EPA, 2017). Figure 1 (CARB, 2017) illustrates that an hour of small engine's run time compares to hundreds of miles of a passenger car. Their environmental impact becomes much more significant when considering their ubiquity. The Outdoor Power Equipment Institute reports that 30 million new general purpose engines were manufactured in 2016 with an estimated 100 million owned in the country (OPEI, 2017). Considering this number is essentially equivalent to the approximately 100 million registered cars in the US, it would seem there should be ample motivation to reduce their impact on atmospheric air quality.

A much more severe concern is the danger these engines pose when operating in close quarters at their allowable CO limit. Between 2004 and 2012, 659 fatalities were caused by the use of general purpose engines due to CO poisoning. Ninety-four percent of those occurred from operating the engines in an enclosed space, but the remaining six percent occurred even with the engine located outdoors. This happens when low velocity wind blows the high concentration engine emissions into houses with minimal mixing and dispersion. This is most common during storm-caused power outages where consumers are tempted to run portable generators near open windows or in open garages if it is still raining. Exposure to CO levels over 70 ppm for extended

periods of time are considered hazardous. Exposure at levels of 150 to 200 ppm and above can cause permanent brain damage or death (CPSC, 2006).

Previous work supported by the US Consumer Product Safety Commission (CPSC) and performed at The University of Alabama to develop a low CO-emission portable generator prototype demonstrated a 93% CO emission level reduction is possible using conventional engine control and exhaust aftertreatment systems (Buyer, 2012). An extension of this effort also included the development of passive methods integrated into the engine control system to detect high ambient CO levels and subsequently shut the engine off under these circumstances (Haskew & Puzinauskas, 2013). The CPSC movement to reduce emissions is likely to be resisted due to cost, so being able to minimize the amount of expensive catalyst mass would help to achieve future goals. The original Buyer (2012) report provides data indicating that near stoichiometric operation of a small, air-cooled utility engine is possible without substantial degradation to longevity, thereby indicating an opportunity for considerable emission reduction through improved fuel control even without the catalyst.

Figure 7. Equivalent emissions for small engines (CARB, 2017)

Engine controls

Traditional (low-technology level) small engines use entirely mechanically based systems for controlling speed, fuel, and spark. Many designs are simplified carryovers from vehicle systems from decades or even a century ago. Without the stringent emissions requirements like vehicles face, the small engines have been able to survive with the mechanical solutions not requiring any further research or design. The following paragraphs discuss traditional engine speed, fuel and spark control that are typical of current small engines on the market. These are followed by a description of electronic systems that control these parameters.

Mechanical Speed Control The traditional method of controlling speed is through a mechanical governor such as the centrifugal flyball governor shown in Figure 2. This device is based on the kinetic energy of weights spinning with a rotational velocity proportional to the engine's crankshaft. A linkage mechanism connects these weights to the engine's throttle. As their rotation speed increases, the weights move outward causing the throttle to close. This arrangement provides proportional engine speed control by balancing the torque produced by the engine with the applied load to the engine. Such a proportional system suffers from inherent speed droop with load. This is because more airflow is required in the engine to increase torque, and to provide the extra air needed to produce the torque, the throttle has to open more which only happens with reduced speed. Increasing the proportional gain (the lever ratio between the balls and the throttle or reducing the spring stiffness (when present) that restrains the flyballs will reduce the droop but will increase the tendency for the speed to overshoot its setpoint. To eliminate the droop and control the overshoot, integral and derivative effects must be incorporated into the mechanism.

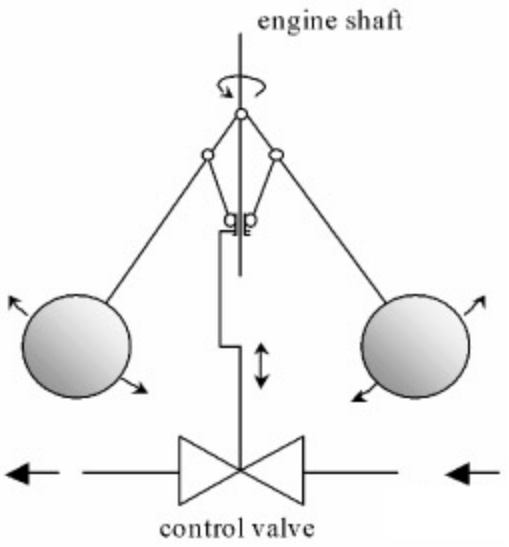

Figure 8. Control schematic for centrifugal governor (Spec, 2006)

Mechanical solutions for the integral and even derivative terms have been designed, but are incredibly complicated and expensive. Figure 3 gives an example of a system that controls proportional, integral and derivative terms and shows the complex mechanical systems it requires.

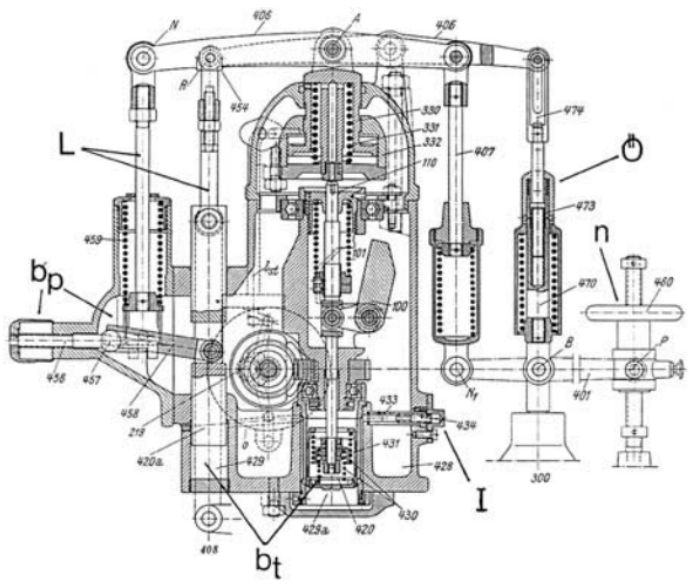

Figure 9. Mechanical governor with proportional, integral, and derivative capabilities (Springer, 1940)

Mechanical Fuel Control. Traditional fuel systems use a carburetor to control the proportion and amount of fuel and air delivered to the engine. Most carburetors primary fuel proportioning occurs using the pressure drop created by passing the entering air through a venturi. A wide variety of auxiliary mechanisms have been developed and implemented on various designs to augment this base fueling rate in order to compensate for transient conditions, high and low load operation as well as cold start. The OEM carburetor which the engine in this study came equipped with was a diaphragm type which is designed for ease of manufacturing and low price. The diaphragm design precludes more sophisticated mechanisms designed to improve fuel control over the engines steady state operating range. It also cannot provide acceleration enrichment either because the metering chamber is sealed from the atmosphere and keeps a vacuum to operate the diaphragm and fuel needle (Woody, 1975). These design choices lead to high fueling error and poor atomization which require overly rich calibration to insure fueling levels never fall below minimum requirements for combustion stability and engine

cooling under all operating conditions. This rich operation leads to high carbon monoxide and hydrocarbon rates as discussed in the motivation section above.

Mechanical Spark Control. Small engines have almost exclusively used a magneto ignition system. While such a system is strictly speaking an electro-mechanical system, the moment when the spark is induced is completely mechanically controlled. The induced spark is created by a magnet installed at a specific location on the engine flywheel (note, this is not the flyweights that are used in the mechanical governor). This magnet then passes under a coil which is fixed to the engine case, and the moving magnetic field energizes the coil. Once the magnet passes, the field collapses and is converted into a high voltage that delivered to the center electrode of the spark plug. If the voltage is high enough to jump the gap from the center electrode to the ground strap, a spark is created that initiates combustion of the fuel air charge trapped in the combustion chamber. This system sparks every revolution of the engine and at effectively the same crankshaft angle every time.

All of the aforementioned mechanical control systems are proven and robust technologies. They don't require any computerization which allows them to be manufactured very cheaply, resist failures, and be easily serviceable if they do need any repair. However, the limited ability to optimize these systems under broad operating conditions prevents significant progress in emission reduction and efficiency improvements. Carburetor-based fuel control system limitations, in particular, could not meet any further reduction in future emission regulations, especially as the engine ages. The fixed magneto ignition system has no spark timing control at all. Consequently, the fixed spark angle is chosen as a compromise for all conditions which often leads to poor combustion phasing at various loads. Finally, the speed control is inherently error-prone as the engine cannot exceed its maximum speed, but must inherently decrease in speed at

load due to its design. The system is also entirely reactive instead of being proactive which amplifies the carburetor's fuel control errors during load changes.

Electronic Engine Control Overview. In contrast to these mechanical counterparts, electronic fuel, spark, and actuator control allow for flexible calibration at all speeds and loads. The fuel delivery quantity and timing is precisely matched with airflow that is either directly measured or calculated from related parameters in order to optimize the fuel-to-air proportion and charge preparation based on operating conditions. The spark phasing can also be easily calibrated to vary through the speed/load range to maximize torque and combustion efficiency. Integral and differential terms can easily be added to electronically controlled and actuated throttles thereby eliminating the inherent droop and substantially improving the response and stability of purely proportional control. All these improvements require additional sensors to measure the relevant parameters and actuators to adjust the controlled variables; however, advances in design and mass production techniques has brought high volume prices of such devices literally to pennies in some circumstances. Electronic systems can also be enhanced with feedback signals to verify if control commands are producing the desired outputs and adjust them accordingly if they are not. These are particularly useful for the fuel and throttle control systems.

The first electronic systems were implementation independently. Electronic ignition systems were incorporated in automotive applications before electronic fuel control systems. Electronic throttle control was first implemented in stationary applications requiring governed speed control such as generators or industrial equipment and was often implemented without electronic ignition or fuel control. Modern systems, however, are fully integrated with either a central computer controller or distributed controllers that communicate with each other. Such coordinated control systems provide extensive opportunities to optimize engine performance. In

particular, and the subject to this effort combined electronic throttle and fuel control implies the control algorithm has a priori knowledge of both the fuel and air flow future and can use that information to prevent over or under fueling during operational transients. In stoichiometric strategies, over fueling will create excess HC and CO emissions while under fueling will create NOx. Minimizing these excursions would be an effective method of reducing emissions.

Fuel control algorithms have been developed to reduce emissions during such rapid load changes, but they have been for multi-cylinder air control. One solution is to use a differential mass flow equation for the intake manifold (Piero Azzoni, 1999) which predicts the airflow change that occurs with changed throttle angle. The differential equation is with respect to crank angle in their research. The change in flow can then be integrated over the entire cycle to determine the total mass ingested by the cylinder. Due to it being a multi-cylinder engine, they are able to determine the throttle change through the rate of pressure change instead of directly monitoring the throttle angle. Single cylinder engines do not have intake manifolds though, and under high load conditions, their entire intake system empties and fills itself multiple times per engine cycle. Mass flow for a single-cylinder engine can be predicted in computer analysis, but it is very complicated and computational intensive (Shun-ichi Akama, 2013). Such a model must be integrated with at least crank angle degree to accurately represent the physics.

Very few OEM electronic control applications have been developed for the small utility engine market sector because of the lenient emissions requirements; however, such technology becomes common as soon as the output crosses the 19 kW threshold. These control systems are expensive relative to the cost of small engines, sometimes almost as much as the engine costs itself. They also require much more development time for calibration than mechanical systems; and this calibration, as described below, presents particular challenges due to the flow dynamics

associated with single-cylinder engines. However, the improved fuel and spark control enable higher combustion efficiencies and increased torque and also lead to a substantial reduction in emissions. Furthermore, the previously cited report by Buyer (2012) indicates that the fuel savings associated with a stoichiometric fuel control strategy will more than pay for this economic cost over the life of the engine.

There are multiple companies that offer aftermarket solutions for small engines, but those are generally for motorsports purposes. The only engines under 19 kW with electronic controls made for non-road purposes is made by Kohler. Their most general-purpose engine is the Command Pro EFI ECH440 which is a 429 cc engine that outputs 10.4 kW (Kohler, 2019). It is used in equipment such as air compressors, blowers, and generators.

The next paragraphs give additional details regarding electronic throttle and fuel control systems given their central role in the present work

Electronic throttle control. Electronic throttle control has fundamentally changed how airflow is used to set an engine's operating condition. Whereas traditionally mechanical systems link to a speed control governor as described above or to a mechanism such as a gas-pedal when direct operator control is desired, modern systems simply monitor the associated outputs of those devices as one of many inputs used to determine the best throttle position. Current automotive systems, for example, use an air-based control strategy with the accelerator pedal position as one of its inputs (Prince, 1998). This strategy assumes pedal is correlated to power and then moves the throttle to match the airflow required preemptively instead of reacting to changing conditions in a reactive system. This helps reduce fueling error and can also provide many other benefits such as torque control and catalyst oxygen storage control. The torque control allows for the engine controller to work more smoothly with transmission controllers during shifts by

determining how much torque must be reduced to provide a smooth shift (Ganoung, 1990). Throttle control on modern systems is very complex due to engine being non-linear. To build a model, engines must be run at thousands of points with various conditions to study the impact of airflow, fuel injection timing, and spark timing. It takes weeks or months to run and analyze, and the model is the top consumer of processing power for the engine controller.

Electronic Fuel Control. Electronic fuel control systems consist of three main components or subsystems that perform the following tasks: 1) Air flow measurement, 2) Fuel delivery, and 3) fuel-air ratio feedback. Air flow is measured using one or more of three standard methods to calculate airflow. The first method, alpha-N, uses throttle angle and engine speed as independent variables to a calibrated airflow lookup table. Its accuracy depends entirely on the calibration and does not adapt to system changes since it relies on that table without any corrections. The next method is speed-density which is based on a similarly calibrated volumetric efficiency table; however, measured manifold air pressure and temperature are used to calculate the density term in the volumetric efficiency definition that yields airflow. Consequently, the airflow calculation incorporates the operating conditions more directly than the Alpha-n method and makes it more robust. Speed-density is the method used in this work, so specific details on how it is implemented are provided in the technical approach section that follows. The last method is a direct measurement of air flow using a hot-wire anemometer and is the most accurate of the three methods. A production automotive airflow sensor cannot respond to rapid changes in air velocity though due to design, so it is only used at steady-state points.

While the latter two methods are considerably more accurate in multi-cylinder engines, there are significant challenges to implement them in one or two cylinder engines. Application is simplified in multi-cylinder engine because there is generally always at least one cylinder

drawing air in from the intake system and the airflow and conditions in the intake manifold are relatively steady. In contrast, the extreme intake and exhaust velocity and pressure fluctuations associated with single-cylinder flow dynamics render the mass airflow meter unusable since the air is moving continuously in alternating directions in the intake port. These pulsations also add a level of complexity to the speed-density method because the pressure downstream of the throttle changes throughout the cycle and the dynamics are different depending on throttle angle. At low load with the throttle nearly closed, the pressure approaches atmospheric during the intake-valve closed portion of the cycle, then drops dramatically during the intake stroke. The associated pressure excursion dampens out rapidly at the throttle. At high load with the throttle near wide open, the pressure excursion alternates as a pressure pulse as it oscillates up and down the runner. This makes it critical to measure the pressure at a very specific point in the cycle to infer load from that measurement. The minimum pressure during the intake stroke gives the best indication of load. Because the point in the cycle at which this occurs varies with speed and load itself, another speed and load dependent table must be calibrated to specify the crank angle at which to make the measurement. This crank angle is known as the 'MAP read angle.' Calibrating this table can be complicated when the manifold pressure sensor is remote mounted and communicates with the measurement runner location with a tube. This has the side effect that fueling is always a cycle behind since the MAP measurement is taken during the intake stroke of the previous cycle.

Fuel Injection. Low-cost systems use a port fuel injector in the engine head pointed at the intake valve. For low emission applications, the injection is timed to occur while the intake valve is closed to allowing the heat of the valve to evaporate the fuel into a gaseous mixture which will burn more efficiently. To maintain this timing in multi-cylinder engines, the injectors must be

able to be independently controlled, which is known as sequential port fuel injection. This is not an issue in a single-cylinder engine. Even with appropriate timing liquid fuel still accumulates on the port walls, which is a significant issue since the amount accumulated varies with load. This means that all the fuel injected for the current cycle may not make it into the cylinder, or conversely, fuel in addition to that injected may enter. Models have been developed to account for this fuel film (Cheng, 2000) to help during transient events as manifold pressure changes. As the pressure changes, the vaporization temperature of the fuel changes leading to the film changing thickness. This can lead to either fuel being deposited or removed from the film and becoming unaccounted for in the fueling control. Injecting while the valve is closed helps to prevent the need to calibrate the complex film model, and it may also be debatable of its usefulness in a single-cylinder engine that varies manifold pressure considerably every cycle.

Electronically controlled fuel delivery is usually monitored using a universal exhaust gas oxygen (UEGO) sensor to infer fuel-air ratio. This sensor is used for feedback control strategies which continuously modify the calculated injected fuel mass to account for conditions unaccounted for in calibration as well as for both short and long-term learning which can compensate for component wear.

Objective

The objective of this study is to develop and evaluate an advanced predictive electronic air and fuel control algorithm for a small single cylinder engine and quantify its performance relative to conventional electronic and mechanical systems typical of commercially available small engines. The performance will be evaluated by comparing the relative air-fuel ratio (lambda) stability and hydrocarbon emissions values during transient load changes.

Technical Approach

This section describes the technical approach used to achieve the objectives stated above. The subsections that follow describe the test engine and dynamometer platform, the advanced algorithm and the additional testing required to characterize the engine intake system's flow characteristics which are used in the predictive control algorithm and the test matrix executed for the investigation.

Test Platform. The engine used for testing is a Honda GX390. It is a 389 cc displacement, 8.7 kW, port fuel injected, four-stroke, air-cooled engine. The combustion system uses overhead valves actuated by pushrods and has a compression ratio of 8.2:1. The test setup is mounted on a heavy table with the dynamometer, and the engine bolted directly to it. The dyno is controlled by an ABB drive that can deliver up to 11 kW. The drive is controlled over Modbus protocol by the same controller that controls the engine. The interface was custom developed in LabVIEW to allow for higher quality control and synchronized data collection since it is an all-in-one solution.

The ECU used is a cRIO from National Instruments with a Drivven package. Drivven is designed to allow for rapid-prototyping of engine control systems. The cRIO is responsible for all inputs and outputs to run the engine. The inputs are intake air temperature (T_{man}), manifold air pressure (P_{man}), throttle position sensor, and the oxygen sensor. The outputs are servo position to control the throttle, fuel injector, and spark driver. The engine controller uses the speed-density method with a MAP read angle mentioned before to control fuel.

The injector used is rated for 102 cc/min at 40 psi and is aimed to inject on the intake valve. It has high impedance, so the fuel injector drive is rated to use a saturated control strategy.

The fuel pressure is controlled by a pressure regulator mounted on the gas tank immediately after the fuel pump and is kept at 40 psi.

ZrO_2 oxygen sensors (are often/typically) used to close the loop on this open loop value. Oxygen sensors use an oxygen concentration cell that generates an electromotive force that corresponds to the oxygen partial pressure difference between what is in the exhaust and the ambient air (Takashi Takeuchi, 1983). These sensors come in two varieties, narrowband and wideband. Narrowband sensor outputs switch rapidly to high or low saturated values when sensing exhaust produced by AFRs respectively rich or lean of stoichiometric and are accordingly often called ‘switching’ sensors. Due to this characteristic, they effectively only indicate a rich or lean state and can’t directly quantify actual AFR. This type of sensor was used in the fuel control system for feedback in this work. The fueling algorithm adjusted the commanded injector pulsewidth based on this feedback to correct deviations from the desired air-fuel ratio. This was accomplished by applying a first-order lag filter to the switching signal which effectively performed a moving average of the lambda signal. This computed average was compared to the desired value retrieved from a second calibrated table based on speed and MAP to establish the current error. The proportional (P) and the integrated (I) value of this error is used to adjust the open-loop injector pulsewidth

Wideband oxygen sensors provide a more linear response to oxygen in the exhaust and are calibrated to measure the air/fuel ratio over a wide range- hence their name. They work based on the same physics as a narrowband sensor but include an oxygen pump which moves oxygen to and from the measurement cell to maintain a stoichiometric mixture. The current is monitored and can be correlated to a lambda value (Tessho Yamada, 1992). This measurement can be collected for data only or as the fuel control feedback signal. Such feedback allows more

accurate and versatile AFR control since errors can be accurately quantified for non-stoichiometric setpoints. Such a sensor was used in this work for data acquisition purposes only.

The method for electronic throttle control on this engine is a servo which allows precise control of the throttle angle and for a proportional/integral controller that can be tuned when desired instead of inherently designed into the hardware. A servo was chosen due to packaging, lack of return spring on the throttle, angular velocity, cost, and ease of use. The mechanical governor is connected to the throttle by a linkage, so this linkage could also be used for the servo. The force required to move the throttle was very little, so a very rapid servo used to gyro control purposes on model helicopters could be used. The servo chosen was a Hitec HS-5085MG which was the fastest servo available with an angular velocity of 0.17sec/60°. Figure 10 shows the controller system for this electronic throttle.

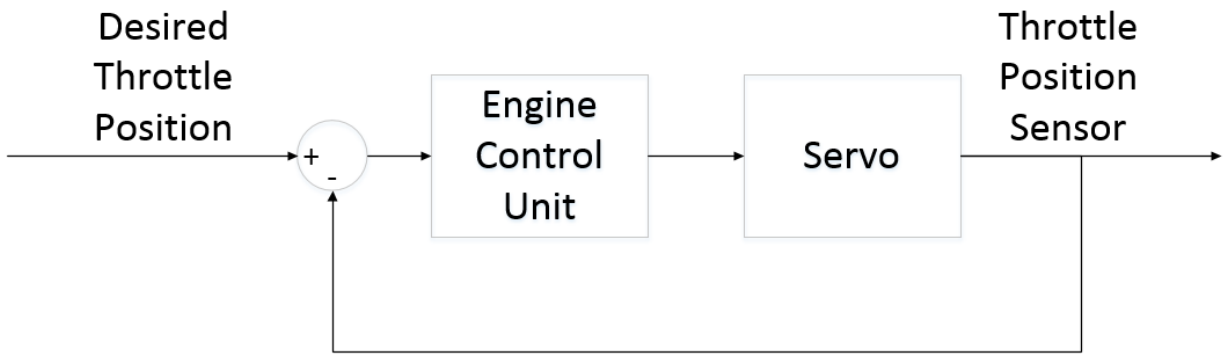

Figure 10. Flow diagram of control system for electronic throttle controller

Due to the nonlinearity of gasoline engine controls mentioned before, the PI controller was calibrated using an iterative process (Shugang Jiang, 2009). The proportional gain was increased until the system went unstable and then the integral gain was increased to dampen and

eliminate the error. Since the throttle PI controller is executed by the engine controller, the flow algorithm has a priori knowledge of the throttle angle at least some finite time before it occurs.

Emissions Analyzer. A Cambustion HFR400 FastFID device was used to measure the hydrocarbon emissions of the engine during tests. This device uses a flame ionization detector in a very small volume mounted as close to the sampling point as possible. It provides a very rapid response rate, around 1 kHz, and outputs it via an analog voltage signal to be recorded by the cRIO. This high rate allows for transient spikes to be captured during load changes. The device has two sampling heads so that one can be placed in each the pre- and post-cat positions, which can then be compared to determine the catalytic efficiency. The device was calibrated before and after every test cycle to verify its readings. This was accomplished using a zero and span gas to set the calibration curve. A complete description of the HFR400's function is provided by Collings (Collings, 1988).

The analyzer outputs mole fraction values, which is typical of most emission measurement instrumentation. This output is adequate for comparing emissions at a fixed load; however, to quantify cumulative results of multiple loads, such as the pattern used in this work as described later in this section, the results must be weighted proportionately to the exhaust molar flow rate. Small engine certification procedures (40 CFR Part 1065) require using a carbon balance or a CVS sampling system with the appropriate analysis to compute total emission mass. The test equipment available for this work did not support such quantification. However, a reasonable estimate was made by assuming the exhaust molar flow rate is proportional to the air-flow rate, which was available here from the cRIO since it calculates airflow to determine fueling. Then, time integrating the product of the mole fraction output and the air-flow rate will

produce a value proportional to the total mass emission and can be used to compare emission performance between various engine configurations, or in this case. control strategies.

Control strategy. A physics-based model was decided to be the optimum method to develop an algorithm. A simple model allows for low computational overhead to be required and requires minimal calibration. The model is based on flow through the throttle which was flow tested on a flow bench, and then the values loaded into the model. The model estimates the next cycle flow and compares it to the previous cycle to modify fueling.

Speed Density. The fueling for the generator used a speed-density algorithm for determining injected fuel mass. Speed-density algorithms utilize the volumetric efficiency (η_{vol}) and a calculated density (ρ_{ref}) to determine the air mass trapped ($m_{trapped}$) in the cylinder:

$$\eta_{vol} \equiv \frac{m_{trapped}}{\rho_{ref} V_D} \tag{8}$$

where V_D is the displacement volume. The reference density is calculated from measured manifold pressure and temperature using the ideal gas law. Finally, the desired air-fuel ratio is used with the calculated trapped mass to determine the fuel that needs to be delivered per cycle under the current conditions can then be calculated:

$$m_{fuel} = m_{trapped} \frac{F}{A_{desire}} = \eta_{vol} \frac{F}{A_{desire}} V_D \rho_{ref} = \eta_{vol} \frac{F}{A_{desire}} V_D \frac{P_{man}}{R T_{man}} \tag{9}$$

where R is the ideal gas constant. The desired fuel-air ratio (F/A_{desire}) and the volumetric efficiency are typically retrieved from look up tables based on current operating conditions defined by engine speed and load. Load was represented with manifold pressure in this application. The final step for the algorithm is to convert the needed fuel to an injector pulsewidth which is calculated based on the flow and response characteristics of the injector:

$$t_{inj} = \left[\frac{P_{man}}{T_{man} * R} * V_D * \eta_{vol}\right] * \frac{F}{A_{desired}} * \left[\frac{1}{\dot{m}_{inj} * \rho_{fuel}}\right] + t_{open} \tag{10}$$

where $\dot{m}_{inj}$ is the fuel mass flow rate through the injector with the current pressure drop and t_{open} is a delay time that compensates for the decreased fuel flow mass flow rate that occurs while the injector opens and closes. As explained above, the manifold pressure must be measured at a specific instant during the intake stroke of the cycle. Consequently, the current cycle's injection pulse width calculation is at best determined on one-cycle old data.

Fuel Injection Modification. The flow prediction algorithm was then implemented by using the empirically calculated throttle flow coefficient ($c_{throttle}$) and then used in the software to calculate the volumetric flow rate (Q) for the previous cycle and the next cycle. The equation for determining flow rate is:

$$Q = c_{throttle}\sqrt{\frac{\Delta P * P_{atm}}{T_{man} * S_g}} \tag{11}$$

where P_{atm} is the atmospheric pressure, ΔP is the difference between atmospheric and manifold pressure, and S_g is the specific gravity of the air. The throttle coefficient characterizes both the area and the flow losses of the throttle. This equation assumes incompressible flow, so the model has limits built in for when throttle angles are low and compressible flow is occurring.

Since cycles are so quick on this engine, temperature and gas properties are considered to be equal between them. This allows for the equation to be slightly simplified and yields the following which provides a flow correction coefficient (K_{flow}).

$$K_{flow} = \frac{c_{throttle,next}\sqrt{P_{man,next}(P_{atm} - P_{man,next})}}{c_{throttle,prev}\sqrt{P_{man,prev}(P_{atm} - P_{man,prev})}} \tag{12}$$

Previous indicates values that were measured. These are the values that would have been solely used to calculate fueling for the next cycle with the traditional fueling method. Next indicates predicted values that will occur during the next intake stroke. Throttle position is just

assumed to meet to the commanded position. When the flow is choked, the correction factor is simply the ratio of the flow coefficients. This coefficient can then be used in the injector calculation to provide a predicted value for the next cycle of the engine.

$$t_{inj} = K_{flow} * \left[\frac{P_{mani}}{T_{mani} * R} * V_D * \eta_{vol}\right] * \frac{F}{A_{desired}} * \left[\frac{1}{\dot{m}_{inj} * \rho_{fuel}}\right] + t_{open} \qquad (13)$$

The following flow chart provides a timing diagram of the process. The flow prediction is calculated first and fed into the mass injection calculation. The MAP read angles are marked with an X during the intake stroke. The prediction is estimating the conditions during the following MAP read angle in the labeled Current Cycle.

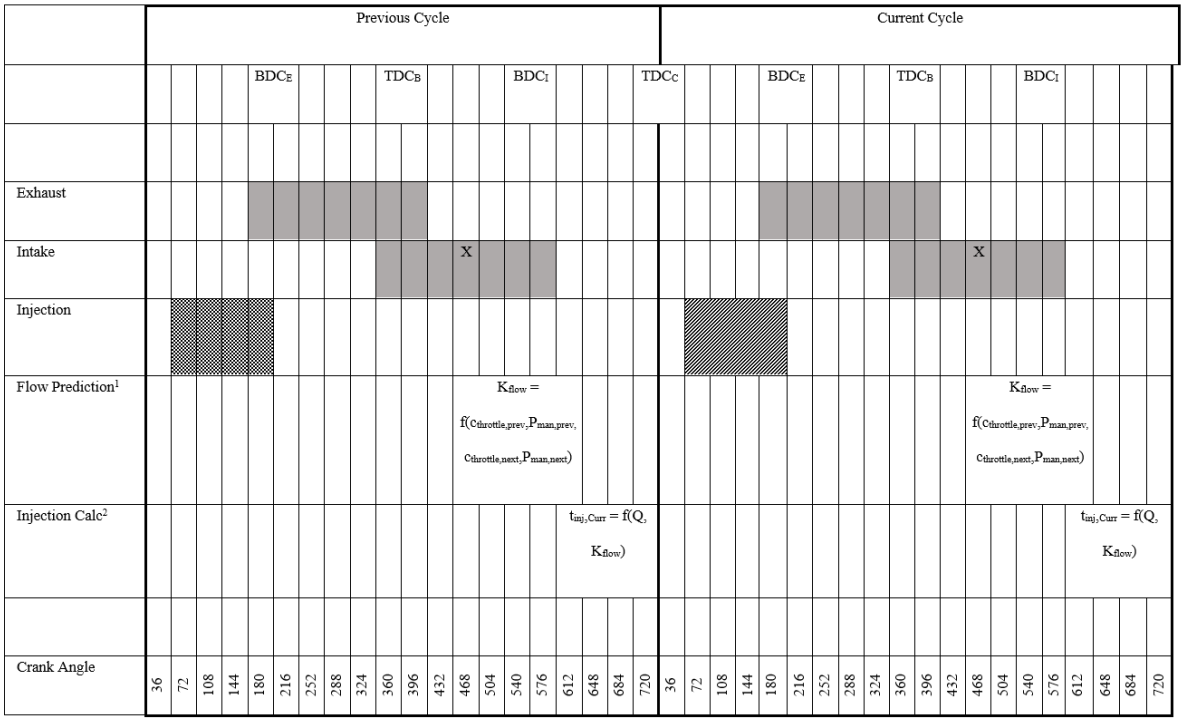

Table 3 Flow chart for two cycles with flow prediction

X –Map read angle

1- Calculated using Equation 5

2- Calculated using Equation 6

Throttle Characterization. This algorithm uses modeled airflow based on data created by measuring actual throttle airflow on a Superflow SF-1020 flow bench. A bellmouth was designed, and 3D printed to be mounted on the throttle to reduce any sharp-edge losses and skew the data. Airflow was recorded while throttle angle and backpressure were varied through expected ranges. The results are seen in Figure 11. The flow coefficients were effectively similar between backpressures, so the flow coefficient could be assumed to be based solely on throttle angle.

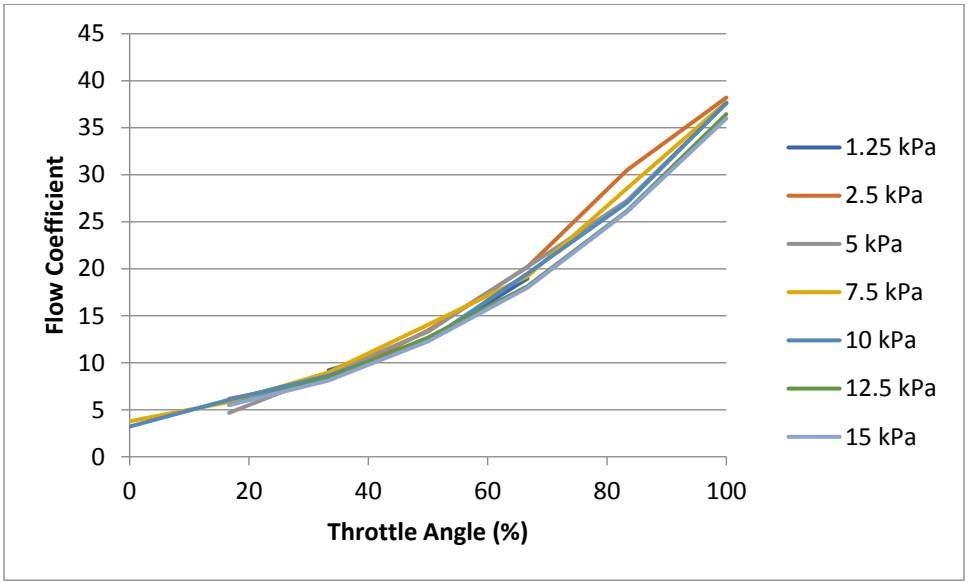

Figure 11. Flow coefficients at various throttle angles and backpressures

Test procedure. The engine was initially calibrated with the electronic throttle on the dyno to allow for any combination of speed and load to be achieved with a stable throttle response when the operating condition is disturbed. Calibration was done by adjusting the VE table to achieve stoichiometric fuel-air ratio at each operating point. Spark was kept constant at 22° BTDC for this experiment. This was the engine's stock, fixed spark setting and was

maintained to simplify the calibration process and evaluation of the transient fuel control effects on engine performance.

A test cycle designed to mimic the normal use of a generator was used to evaluate the various control strategies. This pattern, shown in Figure 12, consisted of load step changes between various levels within the generator's original 5500 [W] capacity. These variable load step changes were intended to focus the control strategy evaluation on transient performance.

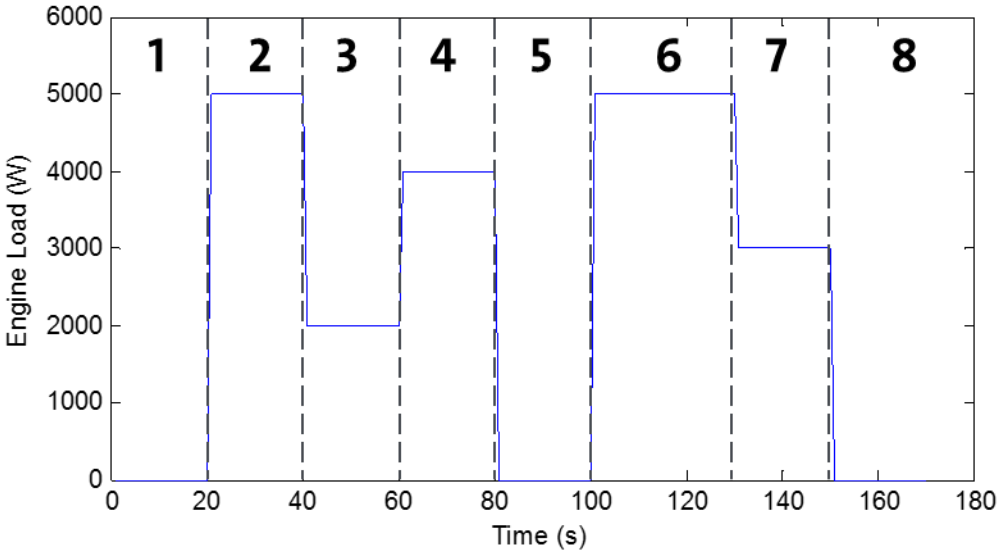

Figure 12. Test cycle used for all tests

The test cycle was run in four different configurations as seen in the test matrix (Table 4). Test 1 is the baseline with the stock mechanical governor and operating in open-loop fueling, which would be the closest setup to production. Test 2 will add closed-loop fueling to study its impact by being able to maintain a stochiometric mixture at all conditions. Test 3 adds the electronic throttle to dampen throttle movement and keep the engine at a constant speed. Test 4 is the full system with the predictive flow control added and will be compared to the baseline to analyze the overall improvement of all components.

	Mechanical Governor	Electronic Governor	Open Loop Fueling	Closed Loop Fueling	Flow Prediction
Test 1	X		X		
Test 2	X			X	
Test 3		X		X	
Test 4		X		X	X

Table 4. Test matrix

Results

This section presents and discusses the results acquired through the execution of the previously described test matrix. The results are presented sequentially, comparing incremental additions to the control capability and strategy with the baseline configuration. This starting point utilized the mechanical governor for speed control and open-loop electronic fuel injection.

The first increment step was to implement closed-loop fueling and compare its performance results to the baseline case. The continuous throttle adjustments associated with the mechanical governor's proportional-only control combined with the reactive fuel delivery response to the oxygen sensor feedback slightly increased the short-term variations in equivalence ratio, as can be seen in Figure 13. However, when observed over a longer time period, the closed loop results stay closer to the stoichiometric target over the broad load conditions tested. This is expected since the closed loop calibration is not perfect even when the engine conditions are closely reproduced and will further degrade with any environmental deviations from the calibration conditions. The closed-loop control system tends to overshoot during transient because of the system staying active. Most automotive systems turn off closed-loop during heavy transients due to the unpredictability and to prevent any wind-up issues.

Sections 1 and 8 are idle points which are inherently difficult to optimize electronically due to the highly non-linear and very high gain air-flow characteristics of a nearly-closed throttle. Consequently, the lambda value variations were large both with and without feedback, but marginally large with the O_2 feedback. Evidently, the feedback could not respond fast enough to the rapid air flow rate changes at the low throttle angles and air-fuel ratio stability is actually better when the high-frequency variations are ignored.

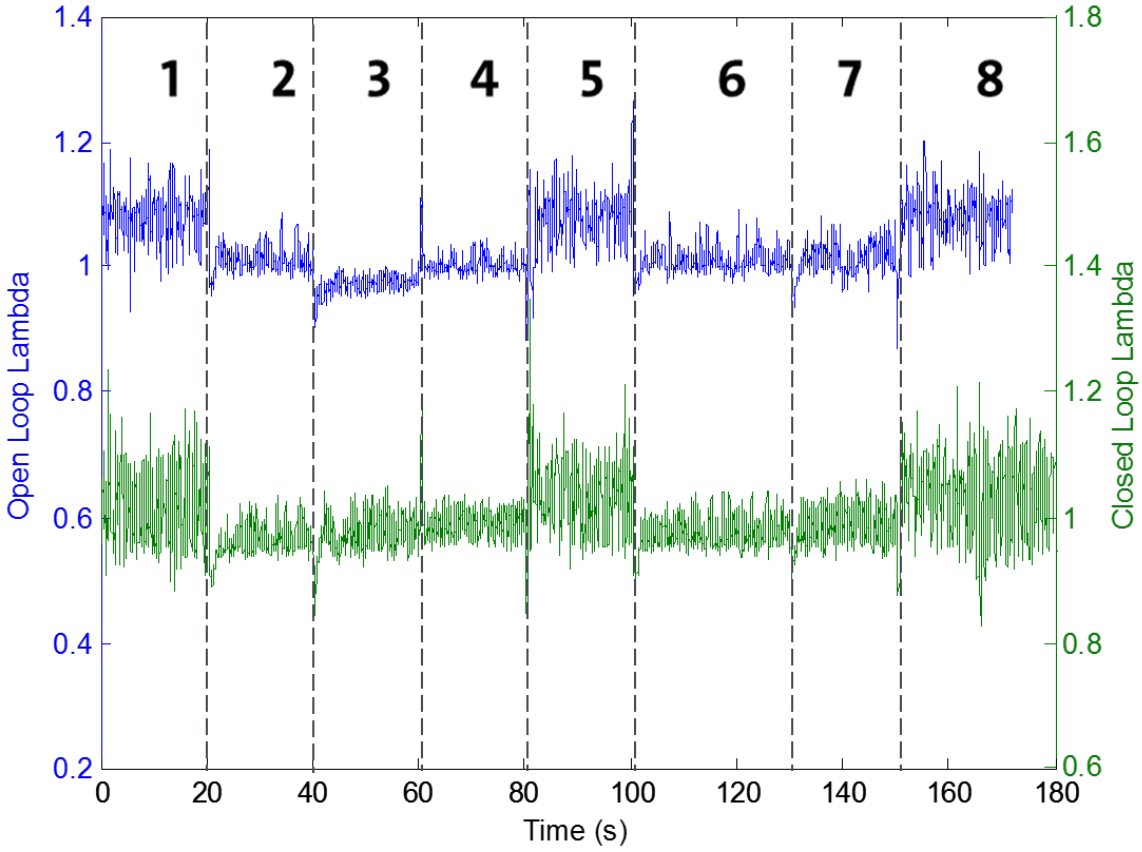

Figure 13. Comparison between open loop (blue) and closed loop (green) fuel control on air-fuel ratio using a mechanical governor during load changes

Closed-loop controlled substantially decreased HC emission under the conditions in which the open loop errors caused rich operation. This is clearly illustrated by the difference in the HC accumulation during segment 3 in Figure 8 the summary in Table 5. Approximately 20%

improvements are evident in both pre-catalyst (solid) and post-catalyst (dashed) integrated emissions.

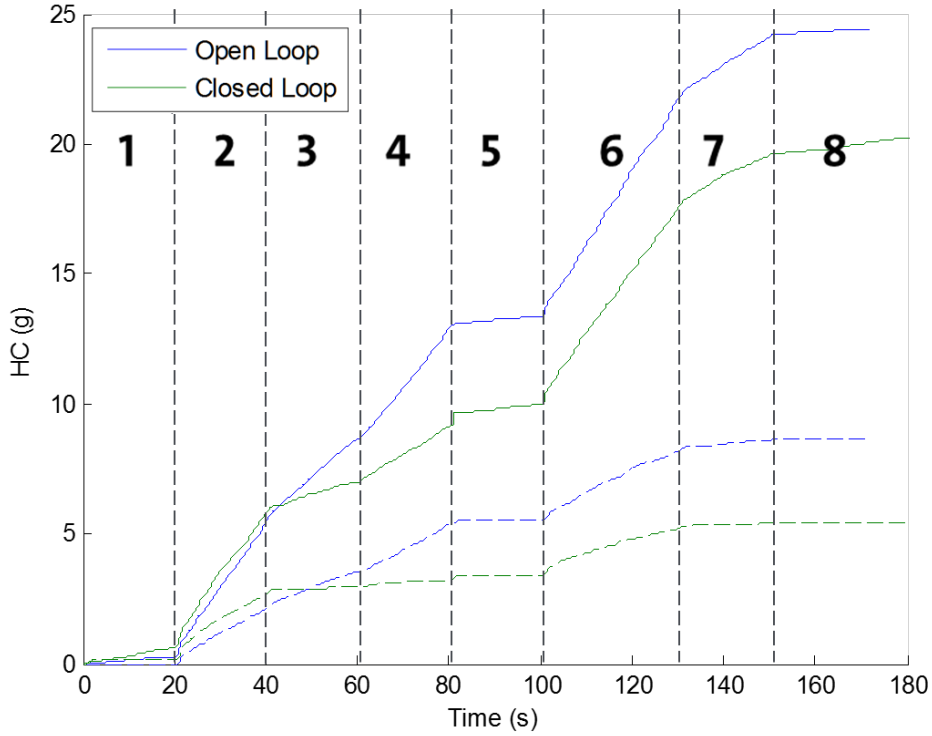

Figure 14. Integrated HC emissions for open loop and closed loop fueling. Solid represents pre-cat and dashed post-cat

The next incremental step was to implement an electronic throttle. The electronic throttle is necessary for the predictive algorithm developed here since the algorithm utilizes the next cycle's anticipated throttle position as one input for the injection duration calculation. This information is inherently known since the algorithm controls the servo which, as described in the background section, is in contrast to the mechanical governor which controls throttle position proportionally to engine speed. The electronic throttle is also able to eliminate the speed droop associated with centrifugal systems, which helps for fueling control as well. The implementation was first done without implementing the predictive control algorithm. After evaluating the

performance with independent throttle and fuel control, the predictive algorithm which integrates the fuel control with the anticipatory throttle position was implemented and evaluated. The respective results are presented consecutively below.

Figure 15 shows a substantial fueling error reduction when using the independently controlled electronic throttle relative to the mechanical governor. The standard deviation of fueling error is reduced by 50% during non-idle points, which reduces HC emissions during steady-state.

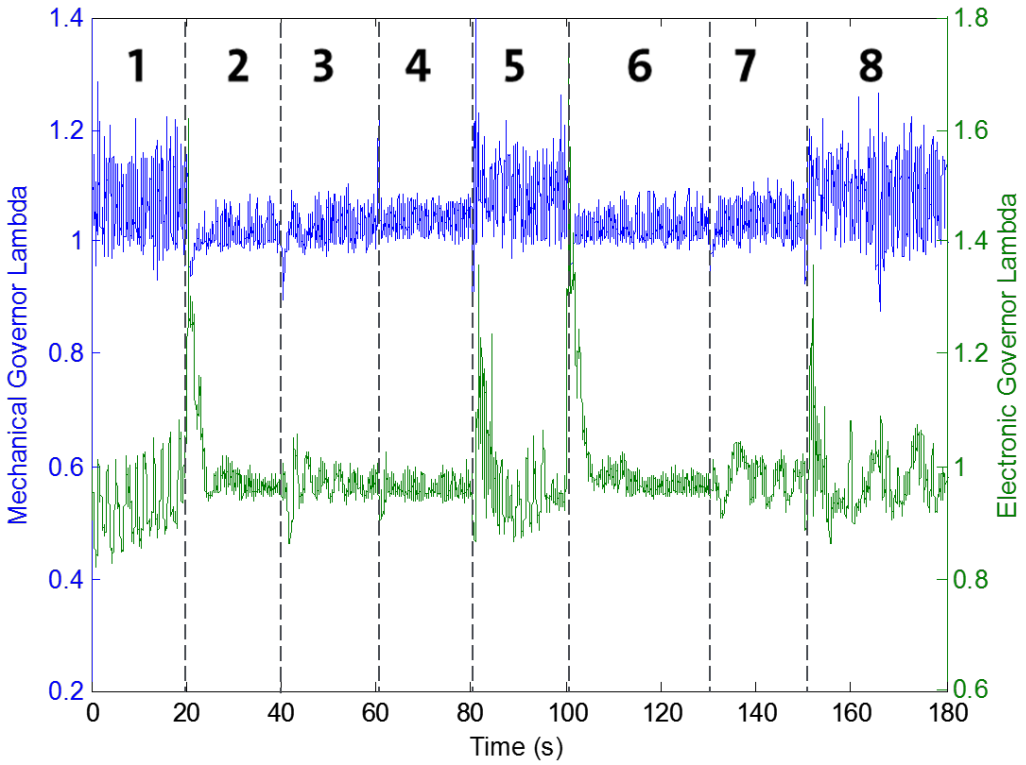

Figure 15. Effect on lambda by implementing electronic throttle. Green is electronic throttle, and blue is mechanical governor

It is noted that the fueling error is actually greater during transient steps compared to the mechanical governor. The electronic throttle controls steady-state points significantly better due to the integral term which virtually eliminates the inherent speed droop associated with the

mechanical governor; however, the response to load changes was slower with the PID gains used in the present configuration. These could have been adjusted to improve the response, but with degradation in stability. These observations are evident in Figure 16 where the steady state speed eventually achieves the 3600 RPM set point in each load segment, whereas the mechanical governor configuration stabilizes more rapidly in each load step, but produces 3700 rpm in the no-load segments (1, 5 and 8) and falls to 3425 at segments 2 and 6, which are the highest load 5000 W cases.

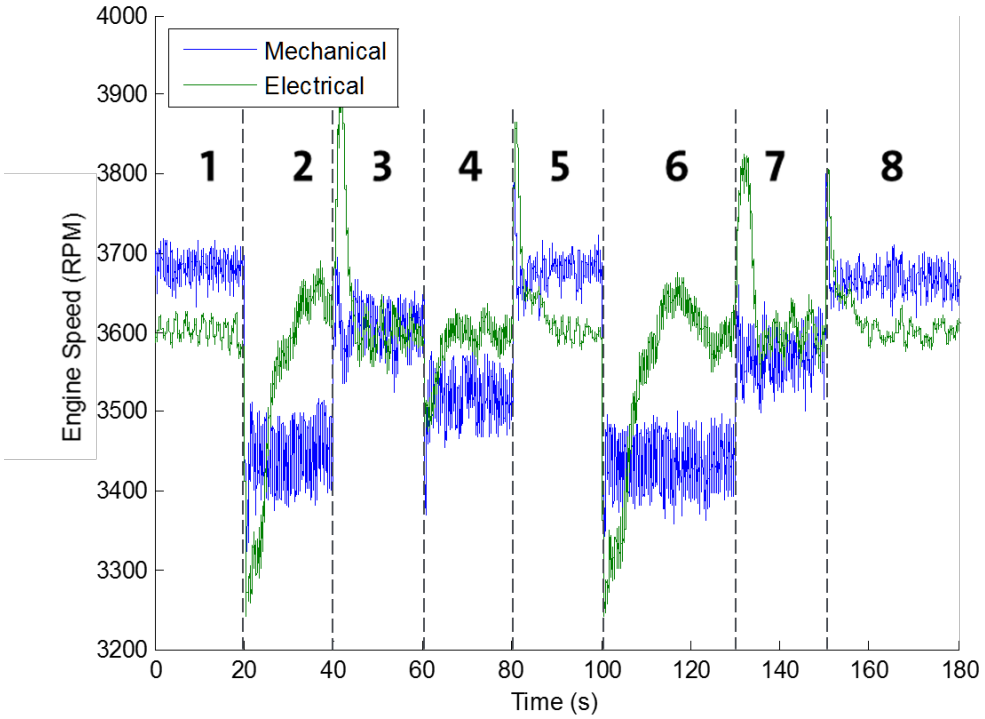

Figure 16. Speed traces for mechanical and electrical governors

Figure 17 shows the impact the following discussions had on the HC emissions. The total pre-cat emissions are lower despite a couple of jumps seen during transients points such as section 5 where misfire likely occurred based on the lambda values. The overall slopes of the pre-cat emissions for the electrical throttle are equal or lower than the mechanical which aligns

with the lower standard deviation for error mentioned before. The post-cat emissions become higher for electrical compared to mechanical though. This is due to the low frequency oscillation visible in the lambda values and will be explained further in the upcoming paragraphs.

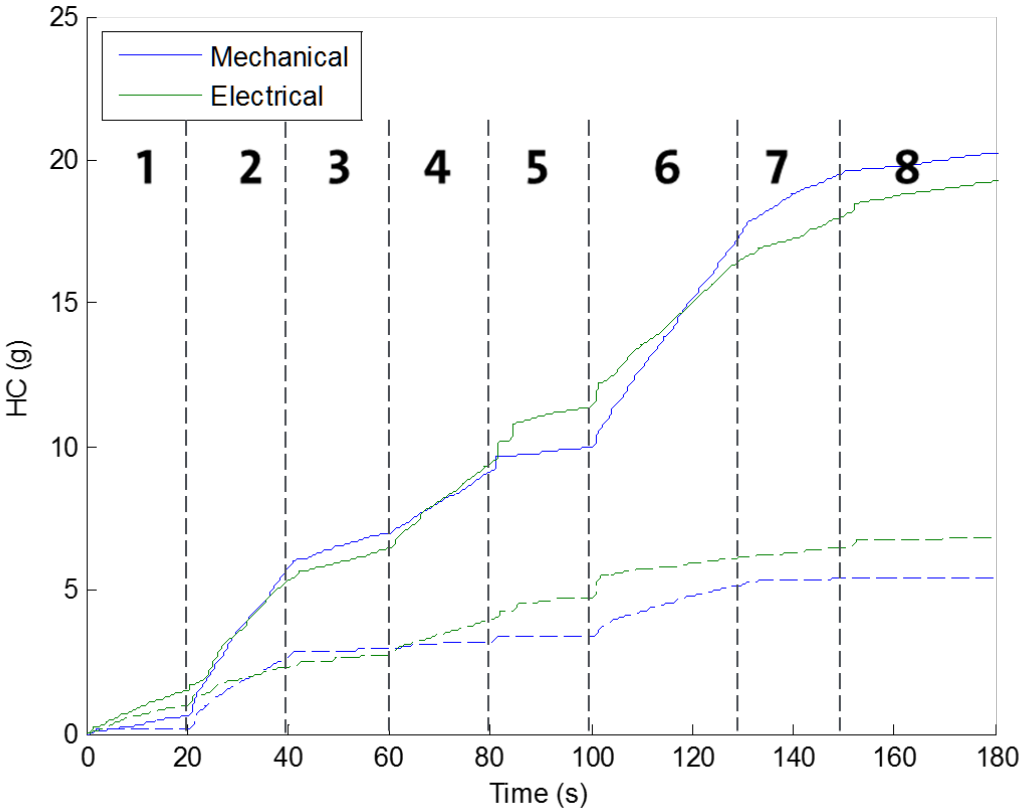

Figure 17. Integrated HC emissions for mechanical governor and electrical governor

The final step was the full implementation of the predictive flow algorithm along with the closed-loop fueling and electronic throttle. The expected areas of improvement were the transients when the throttle is moving the most. Looking in these areas in Figure 18 significant improvements are noted for each step in load. Note that the green trace is the blue trace from Figure 15. The highest impacts are seen when the throttle moves the most, from no load to full load at 20 seconds and 100 seconds. It reduces the fueling error by 73% and 81% in those steps.

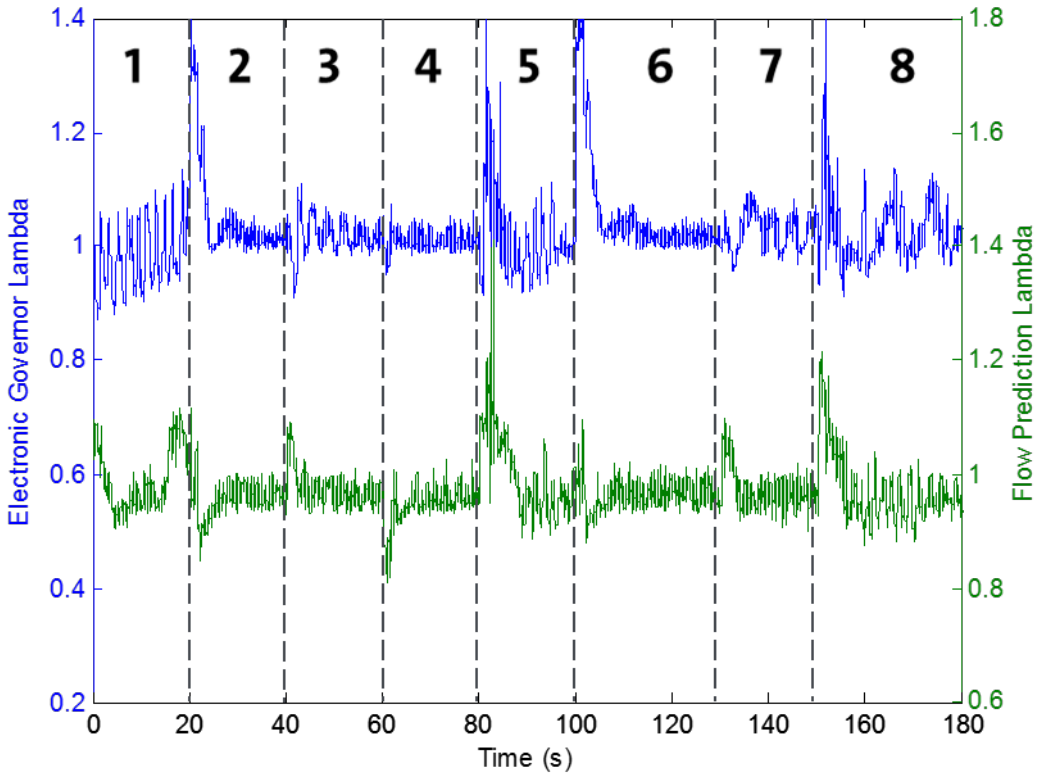

Figure 18. Lambda values for the flow prediction algorithm (green) and without (blue)

A low frequency oscillation can be seen to be eliminated by the flow prediction algorithm, especially in section 3. For a catalyst to work effectively, the mixture must oscillate around stoichiometric between .5-1 Hz (Heywood, 1988). This allows for the oxygen storage and other emissions to accumulate in order for the three-way reactions to occur. Section 3 was analyzed using an FFT to understand its frequency constituents to see that actual impact between tests. The electric governor without flow prediction is seen in Figure 19, and the flow prediction is Figure 20. The FFT without flow prediction shows a very low frequency component which is the oscillations that were noticed. It does have a major component around 1 Hz as well, but it is not the dominant component. This will lead to a less effective catalyst. The flow prediction

eliminates this low frequency component and has its only major peak around 1 Hz, which is ideal.

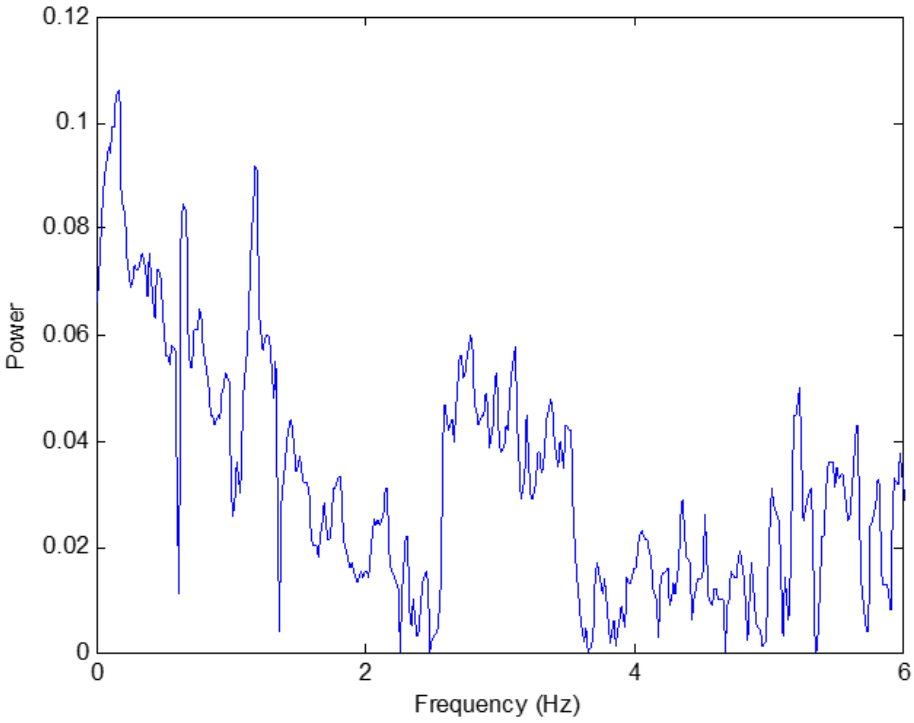

Figure 19. FFT of section 3 without flow prediction algorithm

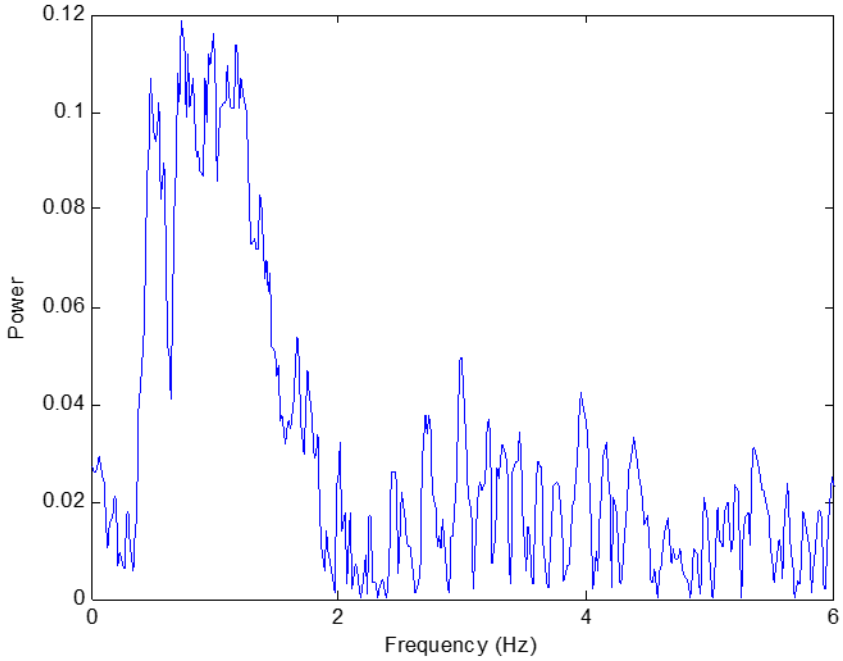

Figure 20. FFT of section 3 with flow prediction algorithm

In the integrated emissions in Figure 21, the overall HC emissions are reduced by a further 17.5% from the closed loop which brings the total reduction to 34% from baseline. This is accomplished through the reduced fueling error during transients as well as the reduced lambda standard deviation as steady-state.

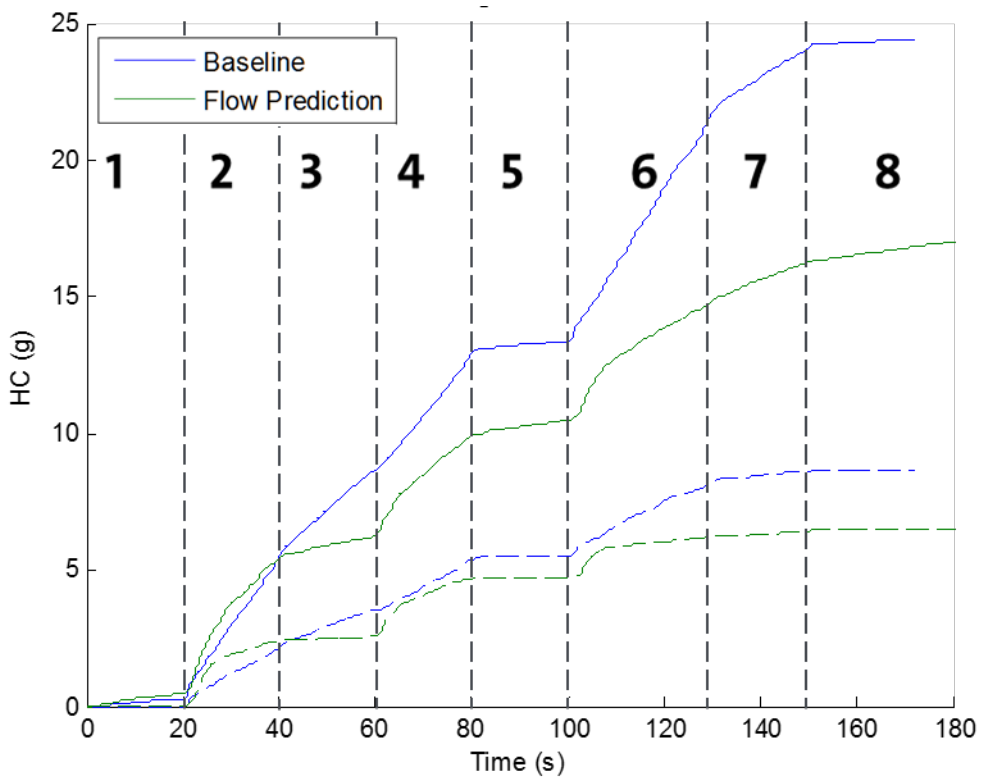

Figure 21. Integrated HC emissions for baseline (blue) and with flow algorithm (green)

The lambda values for each section are summarized in Table 5. The values are calculated once steady-state has been achieved in each section. If the idle sections, 1 and 8, are ignored, and the standard deviation is calculated for each engine setup, then it can be seen that the improved hardware and software reduce fueling error at steady-state by almost a magnitude.

Average Lambda for Steady-State										
	1	2	3	4	5	6	7	8	Standard Dev.	Standard Dev. 2-7
Mechanical open-loop	1.080	1.007	0.975	1.003	1.084	1.008	1.014	1.082	0.040	0.033
Mechanical closed-loop	1.034	0.985	0.999	1.014	1.054	0.996	1.012	1.063	0.026	0.022
Electrical closed-loop	0.991	1.020	1.017	1.007	0.992	1.022	1.028	0.999	0.014	0.012
Flow prediction	1.031	1.002	1.005	0.995	0.997	1.007	1.002	0.983	0.013	0.004

Table 5. Summary of lambda values for each section once steady-state is achieved

Conclusion

The benefits of applying modern electronic engine control to the engine powering a small portable generator were investigated. The electronic system included an electronic throttle actuation which had the primary benefit of eliminating the load-induced speed droop associated with mechanical flyball type governors but also facilitated the possibility of implementing a simultaneous air and fuel control strategy that could potentially reduce emissions during transient operation. The throttle was modeled using a flow bench to determine its flow characteristics as functions of throttle blade angle. These data were incorporated into a simple pseudo-steady flow model of the throttle restriction. This model was used to augment the fuel injection duration to account for the anticipated air flow for the next engine cycle.

Engine dynamometer tests were run based on real-world cycles to evaluate the impact of electronic engine control and the advanced predictive fuel control algorithm for the consumer portable generator market. The results of this study show that electronic throttle control and the advanced algorithm led to significant respective improvements in speed control and transient fueling accuracy which resulted in reduced emissions. Future work can further reduce emissions with smarter closed-loop fueling management, using throttle acceleration rates to determine a more accurate future throttle position, and using a better model to predict MAP.

Significant highlights include:

- Closing the loop on the electronic fuel control using an exhaust oxygen sensor decreased equivalence ratio deviations from stoichiometric by 33% and reduced HC emissions by 20% over the multi-load test cycle.
- Incorporation of the electronic throttle with proportional-integral control virtually eliminates the speed droop associated with simple proportional flyball governors typically installed in this market. The generator unit tested exhibited more than 300 RPM of droop at the maximum 5 KW load compared to the no-load condition with the OEM mechanical governor. While the steady-state droop was eliminated with the electronic throttle, the settling time took as long as ten seconds in the most extreme load transitions, whereas it was nearly instantaneous with the mechanical throttle. It is likely further tuning of the PID parameters or implementation of a more robust throttle control algorithm could reduce or eliminate this discrepancy, but this was not pursued as part of this work.
- Finally, using the fully electronic system (fuel and throttle) the predictive fuel control algorithm improved 66.7% compared to the results using a conventional control strategy. The emission improvement represents a 34% reduction from the baseline open-loop electronic setup. It is worth noting the baseline setup is already a large improvement over the carbureted fueling typical of small engines being sold today.

The gains from the predictive algorithm were achieved without any additional engine calibration beyond what was performed for the closed-loop strategy without predictive control strategy. The only additional work required for incorporating the algorithm was to characterize the throttle flow.

IMPACTS OF CATALYST SIZING AND EXHAUST PULSE FREQUENCY ON CATALYST EFFICIENCY

Introduction

Small, general purpose utility engines are utlized for a wide variety of off-road applications including portable power generators, power-washers, lawn mowers, and portable or handheld lawn, garden and farm equipment. The EPA divides off road engines based on their power output into two categories using a 19 kW threshold. The lower power engines, which are the subject of this work, have significantly higher emission allowances and the consumer market which purchases them does not place a high priority on minimizing fuel consumption. Consequently, their design and development focus is primarily on reducing manufacturing cost and improving reliability and there is limited motivation to incorporate significant technology to lower emissions or fuel consumption. Their development is further simplified when the engine's speed range is limited, which is the case for most of the applications identified above. Homogeneous charge spark ignited combustion systems implemented in a four-stroke cycle are used for almost all but the handheld applications, which often use a two-stroke cycle. Small spark-ignited engines are good choices for the identified portable applications since they are lightweight and inexpensive relative to alternatives such as small diesel engines, gas turbines or fuel cells; however, due to their ubiquity and as is elaborated in the motivation presented below, these small, general purpose utility engines contribute a significant proportion of criteria gas air pollution to the atmosphere. This atmospheric pollution load combined with the proximity of the engine exhaust to the operator in most of the applications suggests that methods to reduce the

emissions and improve the efficiency of such engines warrant serious exploration despite the noted limited regulatory and economic motivation.

This paper describes part of a large comprehensive effort to reduce the emissions of the subset of these engines which are used in portable generator applications (Buyer, 2012) (Haskew & Puzinauskas, 2013) (US Patent No. 9,880,973, 2018). The work described here was performed to test and quantify the effect of exhaust catalyst size in a small single-cylinder engine equipped with an electronic engine control system. The remainder of this introduction provides the motivation for this work, some basic background on catalysts and formally states the objective of this work.

Motivation

Incorporating advanced technology into small utility engines, such as the control strategies described herein, can potentially significantly improve their efficiency and emission performance compared to baseline low-technology engines. Despite this potential, current EPA emission standards for small engines are very lenient relative to those imposed on larger non-road engines. The EPA uses a 19 kilowatt power output threshold to distinguish non-road spark-ignition engines. Table 1 shows allowable criteria gaseous emissions for both engine categories. Of significant note, small stationary engines have practically no CO restriction compared to their counterparts producing 19 kW or above.

	Nonroad Spark-ignition Engine		
	<19 kW		>=19 kW
Year	2005	2011	2007
HC+NOx	12.1	8	2.7
CO	610	610	4.4
	All units g/kWh		

Table 6. Emission standards for small nonroad engines by year

The lax CO standards are primarily driven by economics. To keep their prices low, these engines are almost all fueled using very basic carburetors that have significant manufacturing variability and limited ability to maintain optimum fuel mixture ratio over broad operating conditions. Furthermore, they are practically all air-cooled to eliminate the cost and complexity of liquid cooling systems. Therefore, they typically are set to take advantage of the lenient standard and operate using air-fuel ratios up to 25% rich of stoichiometric. This is done to improve stability during transient operation, compensate for the aforementioned unit-to-unit variability and control combustion temperature. This lenient standard may give the impression that CO emissions from small engines present no health hazard. Perhaps considering that, at least in the US and other first-world economies, toxic atmospheric CO levels are no longer frequent, this may be true. However, the allowable CO emission disparity coupled with the vast number of small engines implemented in lawn equipment, portable generators and a wide verity of other applications mean the total CO emissions from such engines have the potential to easily surpass those from significantly more tightly regulated mobile sources. Consider that a single 5 kW generator currently emits the same amount of CO as up to 625 idling mid-size late 1990s cars (which certainly do not represent the state of the art in emission control) (EPA, 2017). Figure 1 (CARB, 2017) illustrates that an hour of small engine's run time compares to hundreds of miles of a passenger car. Their environmental impact becomes much more significant when considering their ubiquity. The Outdoor Power Equipment Institute reports that 30 million new general purpose engines were manufactured in 2016 with an estimated 100 million owned in the country (OPEI, 2017). Considering this number is essentially equivalent to the approximately 100 million registered cars in the US, it would seem there should be ample motivation to reduce their impact on atmospheric air quality.

A much more severe concern is the danger these engines pose when operating in close quarters at their allowable CO limit. Between 2004 and 2012, 659 fatalities were caused by the use of general purpose engines due to CO poisoning. Ninety-four percent of those occurred from operating the engines in an enclosed space, but the remaining six percent occurred even with the engine located outdoors. This happens when low velocity wind blows the high concentration engine emissions into houses with minimal mixing and dispersion. This is most common during storm-caused power outages where consumers are tempted to run portable generators near open windows or in open garages if it is still raining. Exposure to CO levels over 70 ppm for extended periods of time are considered hazardous. Exposure at levels of 150 to 200 ppm and above can cause permanent brain damage or death (CPSC, 2006).

Previous work supported by the US Consumer Product Safety Commission (CPSC) and performed at The University of Alabama to develop a low CO-emission portable generator prototype demonstrated a 93% CO emission level reduction is possible using conventional engine control and exhaust aftertreatment systems (Buyer, 2012). An extension of this effort also included development of passive methods integrated into the engine control system to detect high ambient CO levels and subsequently shut the engine off under these circumstances (Haskew & Puzinauskas, 2013). The CPSC movement to reduce emissions is likely to be resisted due to cost, so being able to minimize the amount of expensive catalyst mass would help to achieve future goals. The original Buyer (2012) report provides data indicating that near stoichiometric operation of a small, air-cooled utility engine is possible without substantial degradation to longevity, thereby indicating an opportunity for considerable emission reduction through improved fuel control even without the catalyst.

Figure 22.Equivalent emissions for typical lawn equipment

The US EPA currently has no publically announced plans to lower future emission standards for these engines. Motorcycle regulations are currently getting more stringent, but the power rating that is impacted is far above 19 kW. EURO 4 is the closest standard to impact engines around this size engine. Though it is only intended for on-road applications, its regulations include small, low-power output engines for vehicles such as mopeds and scooters (Transport Policy, 2018). Many of these vehicles will require a catalytic converter to meet the new standards. The California Air Resources Board (CARB) is the regulating entity most likely to impose strict enough standards to warrant catalyst incorporation on small non-road engines in the US. They were the first to regulate emissions from such engines, and their standards have led to emission reductions of 40-80% since their original rules were imposed in 1990 (CARB, 2017). They plan on implementing standards that will require a reduction of 80% overall by 2031. This will be achieved through a combination of reductions from small engines as well as expanding the use of electric power for off-road equipment. Small engines will likely require catalytic converters to remain viable under these future regulations.

Catalytic Converters

The following information is a summary from Heck and Farrauto. Engine exhaust emissions reduction efforts typically combine some combination of two strategies. First, the emissions leaving the exhaust port can be reduced through the development of the combustion system and second, these engine-out emissions can be further reduced using an exhaust after-treatment system. Most after-treatment systems incorporate some type of catalytic converter which facilitates chemical reactions which convert the harmful emissions to less toxic or benign species. The following paragraphs describe the global strategy of the two most common automotive catalyst types used in spark-ignition engines. These descriptions are followed by an overview of the materials and structure that facilitates these strategies.

There are two main types of catalytic converters used on spark-ignited engines. The first automotive application used the two-way catalytic converter, which was introduced in 1975 to meet the increasingly restrictive emissions standards in the US. The ‘two-way’ designation stems from its function to remove two criteria emission species from the exhaust- carbon monoxide (CO) and unburned hydrocarbons (UHC). To convert them into less toxic gases, both gases are oxidized using surplus air in the exhaust. In the original applications, the engine would operate in a fuel-rich condition to prevent NOx formation and a crankshaft driven air pump would be used to add air into the exhaust which would be able to oxidize the CO and UHC at the low exhaust temperatures in the presence of the catalyst. This strategy would not be used in modern automotive applications due to the decreased efficiency associates with rich operation and the parasitic loss of the air pump. Two-way catalysts are used today in lean burn applications, however, since by definition the charge inherently contains more than enough air needed to completely oxidize the fuel- preferably in the combustion chamber or in the exhaust aftertreatment system if necessary. In such operation, the charge is either kept lean enough such

that combustion temperatures remain too low for significant NOx production or the two-way catalyst is combined with an additional NOx trap to catalyze the NOx. The global oxidation reactions in a two-way catalytic converter are:

$$2CO + O_2 \rightarrow 2CO_2 \tag{14}$$

$$CH + O_2 \rightarrow CO_2 + H_2O \tag{15}$$

The three-way catalysts were developed a few years later to reduce the efficiency impact associated with two-way air-pump implementations and to meet the US EPA's reduction in allowable NOx emissions from light-duty vehicles that were to be enforced beginning in 1981 (EPA, 2016). As might be deduced, 'three-way' refers to adding NOx reduction to the original CO and HC oxidation of the original two-way catalyst. This additional function significantly increased the complexity of the catalyst design and implementation since oxidation is favored under lean conditions while reduction occurs under rich conditions. Consequently, the engine must operate around stoichiometric fuel-air proportion with carefully controlled rich and lean excursions. It must do this to build reserves for each reaction, as emissions typical when rich (CO and HC) need the emissions that are typical for lean (NO) to react and vice versa. To be effective, the switching frequency around stoichiometric should be around .5 to 1 Hz and fueling deviations as much as 1 AFR can be tolerated in each direction as long as this switching is maintained (Heywood, 1988). In addition to the two-way oxidation reactions shown above, the three-way catalyst adds three NO reduction reactions, which use stored CO, UHC, and hydrogen, respectively:

$$2CO + 2NO \rightarrow 2CO_2 + N_2 \tag{16}$$

$$CH + NO \rightarrow CO_2 + H_2O + N_2 \tag{17}$$

$$2H_2 + 2NO \rightarrow 2H_2O + N_2 \tag{18}$$

Materials. The first component of a catalytic converter is the substrate, which acts as the backbone which the catalyst materials are placed upon. It must be an inert material that can withstand the extreme environment it works in. Ceramic is generally chosen due to its ability to function in high temperatures and its ability to be easily extruded into many shapes. A honeycomb design is used due to its high surface area per unit volume taken up in the airflow. The airflow must be as unimpeded as practical to prevent additional backpressure on the engine but must have enough surface area to successfully treat the emissions. In extreme temperature situations, metal substrates are used with the negative of a high manufacturing cost.

The washcoat is the second component of a catalytic converter. It is another inert material that the catalyst is suspended within. Its purpose is to provide a method to apply the catalyst to the substrate with the maximum surface area possible. To do this, it creates a very porous finish. Materials typically used as the washcoat include aluminum oxide, titanium dioxide, silicon dioxide, or a mixture of silica and alumina.

The catalysts come in the form of three rare metals: platinum, palladium, and rhodium. These are very expensive and rare metals so designers must optimize every aspect of the catalyst design to reduce the mass required. Platinum is generally the most common material used as it can both oxidize and reduce the emissions. Palladium can only oxidize, and rhodium can only reduce, so the two are generally used in tandem.

To effectively process the emissions, a steady flow of exhaust gas is needed to build reserves of the necessary constituents for each reaction. Multi-cylinder engines are very helpful in this aspect because they effectively are continually flowing from the effect of at least one cylinder blowing down exhaust throughout the engines revolution. A single-cylinder engine adds complexity though with flow occurring both directions since the exhaust pulse only lasts for

about 25% of the time. This leads to stagnant emissions, processed emissions, and possibly fresh oxygen from after the exhaust pipe flowing over the catalyst multiple times per cycle which requires a larger mass of catalyst to be able to cope with the additional residence time.

Objective

The objective of this study is to analyze and compare the efficiency of a catalytic converter based on total catalyst mass. The results will be compared between a single-cylinder and a multi-cylinder engine to determine the impact of exhaust pulse frequency on efficiency as well. The performance will be quantified with hydrocarbon emissions measurements.

Technical approach

This section describes the technical approach used to achieve the objectives stated above. The main goal was to test the impact of catalyst mass on emissions to compare the efficiency of a single-cylinder against a multi-cylinder engine. The subsections that follow describe the catalyst used, the test engine and dynamometer platforms, the air-metering strategies used in both engines and the emission measurement equipment used for the experiment.

Catalyst. The catalyst used in this research is a 14.4:1 ratio of palladium to rhodium. The cartridge has a diameter of 71 mm and a height of 37 mm, or a volume of 150 cubic centimeters. The density of the catalyst material is 3.6 kg/L resulting in a total of 9.5 grams of catalyst in each cartridge. All three catalysts have the same density of catalyst, so the mass will vary proportionally with volume. There will be three cartridges used at a maximum and one at a minimum.

A custom holder was designed and manufactured to hold the catalysts shown in Figure 23. The catalysts were cylindrical cartridges which easily allowed for changing the total catalyst

volume. The housing was machined from stainless steel and able to hold three cartridges or spacers depending on the volume of catalysts desired. The ends were then attached to quick-disconnects for the exhaust to be able to change the cartridges easily. The housing also had multiple taps added for emissions sampling before and after each catalyst cartridges to analyze their impact.

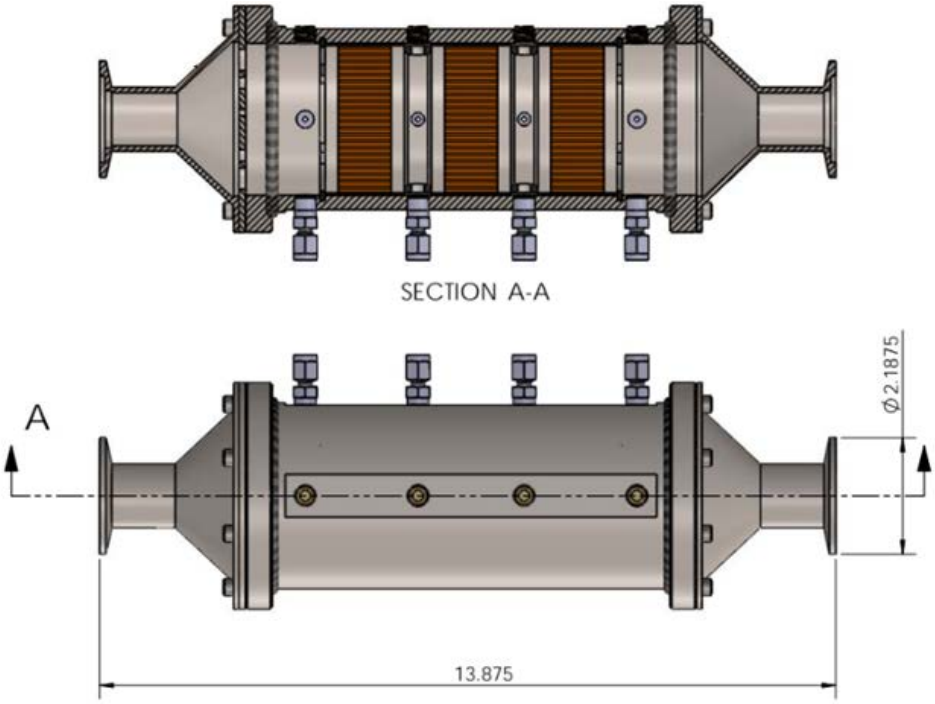

Figure 23. Technical drawing of the custom catalytic converter housing

Single-cylinder engine. The single-cylinder engine used for testing was a Honda GX390. This engine is air-cooled with a 389 cc displacement. Its OEM carburetor was upgraded to an electronic port fuel injection system. A National Instruments cRIO embedded real-time computer equipped with an FPGA, digital and analog input and output and serial communication modules were used for engine control unit (ECU), dynamometer command and data acquisition functions. The 15 HP AC dynamometer was connected to the engine using a driveshaft with XXX couplings and was controlled by an ABB four-quadrant variable speed drive (VSD). A

LabVIEW virtual instrument (VI) was developed in-house to interface with the VSD. The VI-VSD communication was done using Modbus protocol through the serial hardware module in the cRIO system.

The ECU functions were implemented using the National Instruments Drivven package. Drivven is designed to allow for rapid-prototyping of engine control systems. The cRIO is responsible for all inputs and outputs to run the engine. The inputs are intake air temperature, manifold air pressure (MAP), throttle position sensor, and the oxygen sensor. The outputs are servo position to control the throttle, fuel injector pulsewidth, and timing, and spark driver dwell and timing. The pulsewidth was calculated to deliver the appropriate amount of fuel to achieve a stoichiometric proportion to the air flow through the cylinder. The speed-density strategy with proportional-integral (PI) switching O_2 feedback (described in detail below) was used for this calculation.

The modular catalytic converter is installed 8.3” after the exhaust valve as seen in Figure 24. The narrowband and wideband sensors are installed in the exhaust pipe between the engine and catalytic converter.

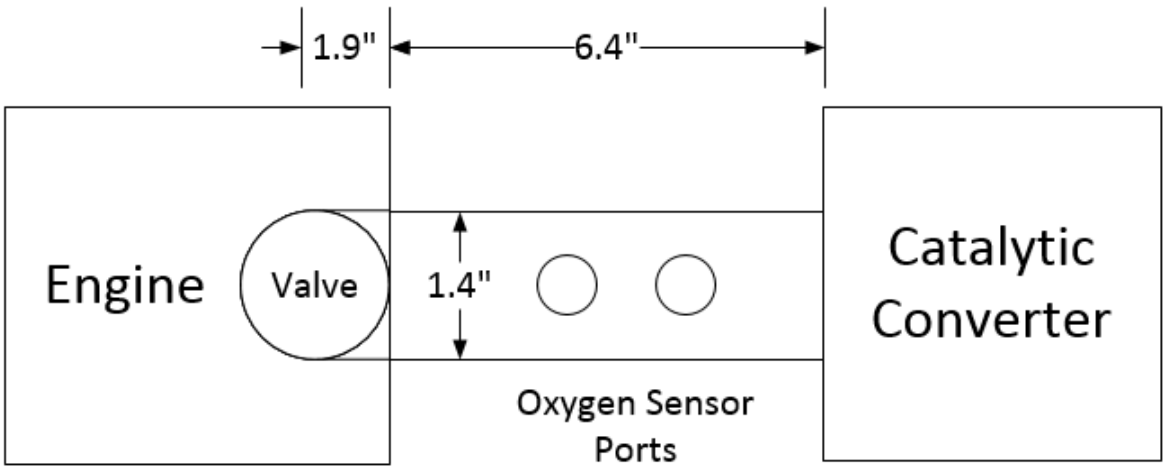

Figure 24. Schematic of the single-cylinder exhaust system

Multi-Cylinder Engine. The multi-cylinder engine used is a Chrysler 2.4 L four-cylinder, naturally aspirated, port fuel injected engine. The engine speed was controlled by a 100 HP GE DC dynamometer connected to the building power through a Dyne Systems solid-state four-quadrant controller. The load was controlled through throttle position that was fixed by a throttle servo motor. Both the four-quadrant controller and throttle servo motor were controlled a Dyne Systems Interloc 4 digital engine setpoint controller

The ECU used for this engine is a Megasquirt 3 open-source controller. It provides many benefits, especially for research purposes. This revision has many of the same features as much more expensive controllers, but also provides the code and compiler to allow for modifications. It can support fully sequential fuel injection, ignition coil control, and control many logic outputs. The software allows for custom calibrations and even provides extra tables to be able to modify outputs. It also uses a speed-density fueling algorithm similar to the Drivven system, in which the ideal gas law is used along with the volumetric efficiency to determine the mass of air in the cylinder. The fuel injection is then based on this and the enrichment desired. An NTK wideband oxygen sensor was used for the closed-loop feedback.

The catalyst on this engine could not be as closely coupled as the single-cylinder engine. The total distance is 36” from the exhaust valves to the catalytic converter and also has the oxygen sensors between the engine and catalytic converter as seen in Figure 25.

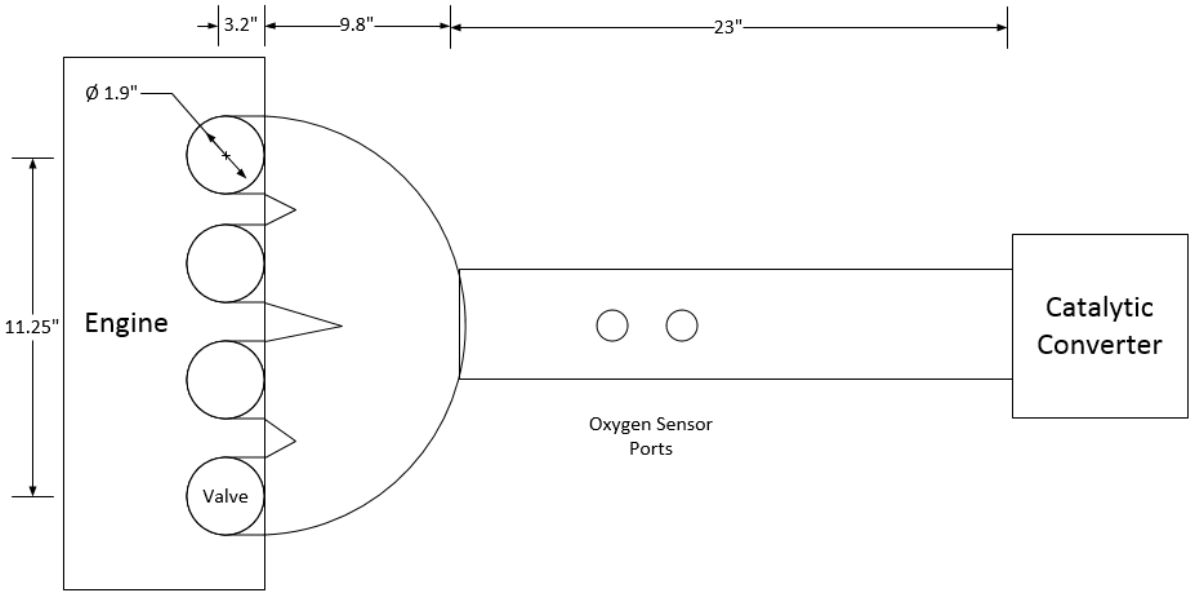

Figure 25. Schematic of the multi-cylinder exhaust system

	Single-cylinder	**Multi-cylinder**
Manufacturer	Honda	Chrysler
Year	2006	1995
Displacement	389 cc	2.4 L
Cylinders	1	4
Stroke	4	4
Valvetrain	OHV	DOHC
Injector Location	Port	Port
Peak Power	11.7 HP	140 HP
Compression Ratio	8.2:1	9.4:1
ECU	Drivven	Megasquirt 3

Table 7. Comparison of key engine attributes

Speed-Density Fuel Control. Both engine controllers used a speed-density fuel control algorithm with O_2 PI feedback. Such algorithms are well-known and have been well-described in

many sources, most recently by Reif (Reif, 2015). This summary is included for completeness. Speed-density algorithms utilize the volumetric efficiency (η_{vol}) and a calculated density (ρ_{ref}) to determine the air mass flow rate into ($\dot{m}_{air,in}$) the engine:

$$\eta_{vol} \equiv \frac{\dot{m}_{air,in}}{\rho_{ref} V_D \frac{N}{n}} \tag{19}$$

where V_D ,N and n are the displacement volume, engine speed and number of revolutions per cycle, respectively. The reference density is nominally calculated from measured manifold pressure (MAP) and temperature (MAT) using the ideal gas law; however as described below, the measurements and implementation are highly dependent on the cylinder configuration. The 'speed-density' designation implies that the air flow rate only depends on the manifold density and the engine speed. Under ideal circumstances, this could be true if the volumetric efficiency only depended on engine speed:

$$\dot{m}_{air,in} = \eta_{vol}(N)\rho_{man}(P_{man}T_{man})V_D \frac{N}{n} = f(N, \rho_{man}) \tag{20}$$

Engine speed is, in fact, the primary influence on volumetric efficiency as the flow losses, and the intake charge's associated inability to keep up with the piston motion depends mostly on the flow velocity. However, loss coefficients are known to depend on Reynold's number, which depends on the fluid density as well as velocity. Furthermore, quantifying the appropriate manifold density is not as straightforward as it may seem- particularly in engines with one or two cylinders. Figure 26 compares typical manifold pressure histories at two different loads from an in-line four cylinder and a single-cylinder engine such as the two used in this study.

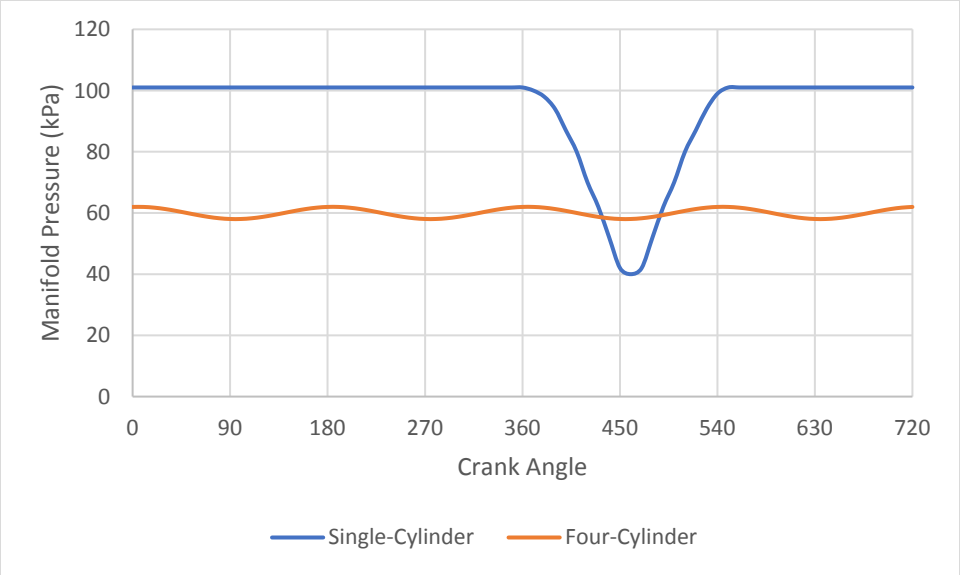

Figure 26. Single-cylinder and four-cylinder manifold pressure traces

It is clear from this figure that the strategy to measure and process MAP should differ in the two engines. Because the oscillations are much less dramatic and the cyclic average pressure is proportional to load in the four-cylinder trace, the MAP can be read with a slow response transducer and filtered with time constants on the order of one cycle. This strategy would not work in the single-cylinder engine because the manifold is only being drawn on for about a quarter of an engine cycle. Consequently, the intake pressure remains near atmospheric while the intake valve is closed and then drops to its lowest pressure somewhere around the point of maximum piston velocity on the intake stroke. Because the net flow rate does increase at high load, the pressure will be slightly lower in the mean during the valve closed portion of the cycle, albeit with higher fluctuations than the low load case. This is the opposite of what happens in the mean over the entire four-cylinder cycle where higher load means a lower pressure drop across the throttle and therefore higher manifold pressure. A much better indicator of load in the single-cylinder is the minimum pressure that occurs during the intake stroke, which follows the

conventional relationship with load. However, since the minimum pressure occurs during a brief trough in the trace, it is critical to measure the MAP at the appropriate engine crank angle to capture the lowest pressure in the system. This minimum pressure location, called the MAP read angle (MRA), is experimentally determined and indexed in a calibration table as a function of engine speed and load. Since load is determined by the correspondingly measured pressure, the table is actually recursive, making it extremely sensitive to measurement or calibration error. The measured pressure is then combined with the air intake temperature using the ideal gas law to provide a correlative quantity to the mass of the air in the ideally full cylinder. The volumetric efficiency is then applied using this quantity as explained above to estimate the actual air mass trapped in the cylinder at intake-valve closing (IVC). Several factors, including flow losses, intake dynamics, and parametric errors make the correlative ideal-gas quantity deviate much more significantly from the actual trapped mass in a single-cylinder engine than it would in a four or higher cylinder count engine. The parametric errors are primarily due to inaccurate representation of the cylinder temperature and pressure at intake valve closing. The measured pressure, in particular, deviates significantly from the IVC value in the single cylinder. Whereas the lowest *manifold* pressure occurring during the intake process has the best *correlation* to air flow rate than MAP values measured at any other point in the cycle, it would not be expected to equal the pressure *in the cylinder* almost half a crankshaft revolution later. It is theoretically possible to analytically determine systematic relationships between the measured manifold and IVC pressures as well as the other noted deviations in the ideal gas quantity. However, establishing these systematic relationships is extremely complex and requires experimental validation. Consequently, the volumetric efficiency is typically experimentally calibrated and,

similarly to the MRA, indexed in a table with engine speed and load (based on MAP) as the independent variables.

Once the air-flow rate is determined, the algorithm uses the injector flow-rate and opening and closing characteristics to determine the opening duration that would be expected to result in the desired air-fuel ratio. In this study, that air-fuel ratio was always stoichiometric; however, the desired air-fuel ratio is typically also tabulated using independent speed and load variables to optimize the value based on engine operating conditions. A closed-loop feedback is added to adjust the pulsewidth to correct for possible calibration or measurement errors or any system degradation.

ZrO_2 oxygen sensors (are often/typically) used to close the loop on this open loop value. Oxygen sensors use an oxygen concentration cell that generates an electromotive force that corresponds to the oxygen partial pressure difference between what is in the exhaust and the ambient air (Takashi Takeuchi, 1983). These sensors come in two varieties, narrowband and wideband. Narrowband sensor outputs switch rapidly to high or low saturated values when sensing exhaust produced by AFRs respectively rich or lean of stoichiometric and are accordingly often called ‘switching’ sensors. Due to this characteristic, they effectively only indicate a rich or lean state and can’t directly quantify actual AFR. This type of sensor was used in the fuel control system for feedback in this work. The fueling algorithm adjusted the commanded injector pulsewidth based on this feedback to correct deviations from the desired air-fuel ratio. This was accomplished by applying a first-order lag filter to the switching signal which effectively performed a moving average of the lambda signal. This computed average was compared to the desired value retrieved from a second calibrated table based on speed and MAP

to establish the current error. The proportional (P) and the integrated (I) value of this error is used to adjust the open-loop injector pulsewidth

Wideband oxygen sensors provide a more linear response to oxygen in the exhaust and are calibrated to measure the air/fuel ratio over a wide range- hence their name. They work based on the same physics as a narrowband sensor but include an oxygen pump which moves oxygen to and from the measurement cell to maintain a stoichiometric mixture. The current is monitored and can be correlated to a lambda value (Tessho Yamada, 1992). This measurement can be collected for data only or as the fuel control feedback signal. Such feedback allows more accurate and versatile AFR control since errors can be accurately quantified for non-stoichiometric setpoints. Such a sensor was used in this work for data acquisition purposes only.

Emissions equipment. A Cambustion HFR400 FastFID device was used to measure the hydrocarbon emissions of the engine during tests. This device uses a flame ionization detector in a very small volume mounted as close to the sampling point as possible. It provides a very rapid response rate, around 1 kHz, and outputs it via an analog voltage signal to be recorded by the cRIO. This high rate allows for transient spikes to be captured during load changes. The device has two sampling heads so that one can be placed in each the pre- and post-cat positions, which can then be compared to determine the catalytic efficiency. The device was calibrated before and after every test cycle to verify its readings. A complete description of the HFR400's function is provided by Collings (Collings, 1988).

Both engines were calibrated to run at stoichiometric and with sufficient spark in the ranges to be tested. The single-cylinder was run at 3600 RPM and up to 5 kW in 1 kW steps. The multi-cylinder engine had its load determined by running the same airflows as seen in the single-cylinder to provide a better comparison between engines. The various airflows were run at

fractions of 3600 RPM to find which were feasible before becoming unstable. The lowest loads were not able to be achieved, but 3-5 kW equivalent were stable. The speeds chosen to compare were 900 and 1800 RPM. The 900 RPM will provide the same amount of pulses for an equivalent airflow as the single-cylinder engine, and the 1800 RPM will deliver twice as many. The engines were run at each point until the system became steady regarding temperature and fuel control. Higher speeds could not be run without running into stability issues due to extremely low throttle angle.

Results

Temperature. A catalyst must reach a certain temperature to be functioning, often known as a "Light-off" temperature. The efficiency varies with temperature and depends on the catalyst material used. Figure 27 (Farrauto, 2002) shows the efficiency of the catalyst used in this test at various exhaust temperatures and also shows the zones in which each engine was operating. Red represents the multi-cylinder range, and blue is the single-cylinder. The temperature was measured in the catalytic converter housing. The multi-cylinder operates just above the effective temperature while the single-cylinder is far above the minimum temperature. The lower temperatures seen in the multi-cylinder testing is likely due to the better combustion system as well as the distance from the exhaust valve to the catalytic converter housing. Catalysts must be broken-in, or aged, at high temperatures to become fully stable. Each of these catalysts was run for a minimum of 10 hours upon receiving them from the supplier to meet the specifications.

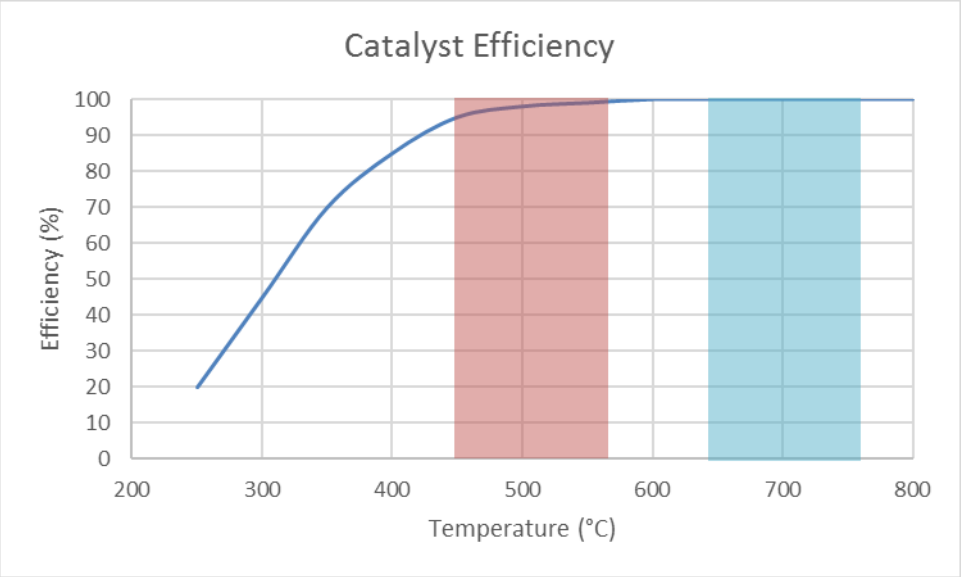

Figure 27. Efficiency curve for Pa/Rh catalyst and temperature regions for each engine

Pressure. The exhaust pressure for each setup was also recorded at the pre-cat location. The pressure fluctuations were expected to be greater for the single-cylinder with the ripples being reduced on the multi-cylinder with increased engine speed. The pressure fluctuations are a good indicator of flow and if any reversal is occurring. The pressure was measured with a Kistler 4049A pressure transducer, amplified with a Kistler amp, and measured with a Tektronix DPO4034 350 MHz oscilloscope. Figure 28 shows the data of the single-cylinder at 3600 RPM and the multi-cylinder running at 900 RPM and 1800 RPM all with equivalent airflow. The single-cylinder exhaust pressures have extreme peaks and go below atmospheric pressure indicating a likely reversal in exhaust flow. The multi-cylinder has two lines plotted: one at 900 RPM, having equal pulse timing at the single-cylinder at 3600 RPM, and 1800 RPM showing twice the frequency. The pressure is significantly smoother for both speeds compared to the single-cylinder with decreased peak-to-peak pressure with the increased engine speed.

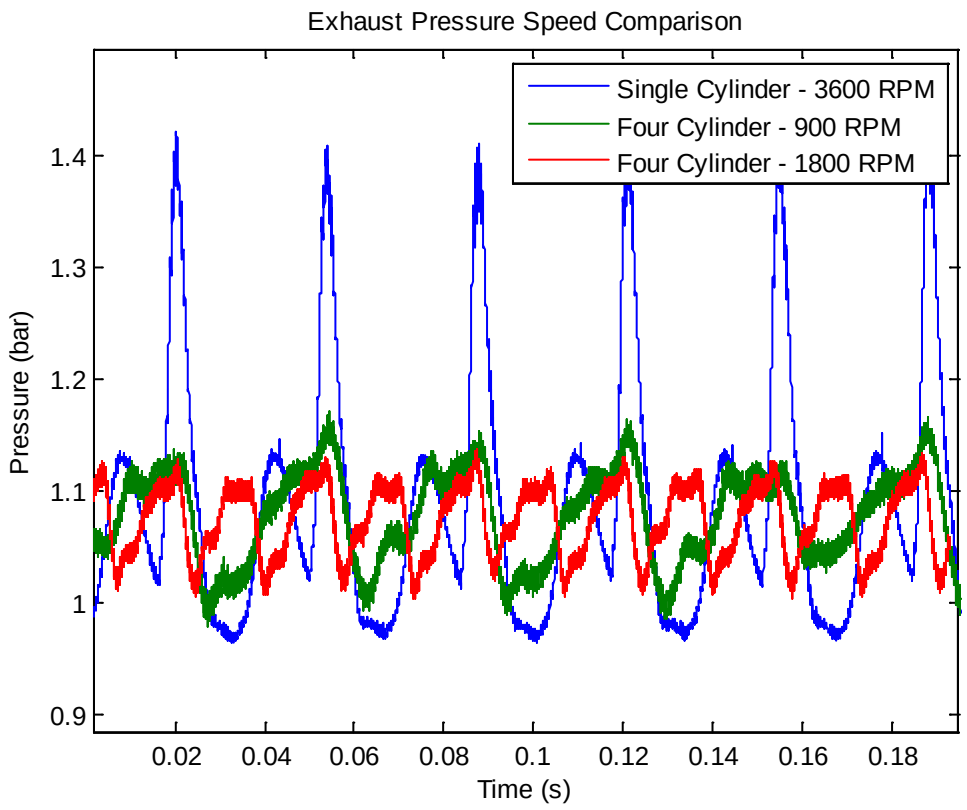

Figure 28. Exhaust pressure measurements for both engines

Emissions. Figure 29 shows the efficiency of the catalysts calculated from hydrocarbon conversion at various loads and grouped by the number of catalyst cartridges used. The trend shows that efficiency generally decreases inversely of load, which is to be expected with the increase of exhaust flow and emissions and the catalyst not having enough mass to capture and process them. The efficiency increases with the introduction of additional catalyst mass until it reaches a point of diminishing returns with the highest mass setup. The addition of any more cartridges than three would likely yield minimal if any improvement.

The general rule of thumb for engine sizing is to make the catalytic converter 50-80% of the volume of the engine. One study examined the effects of catalyst sizing on a small engine,

but with a carbureted engine (Pan-Hsiang Hsien, 1992). Their engine was 125 cc, and they tested two catalyst volumes that were 48% and 87% the volume of the engine. This is comparable to the lower two volumes in the current study which are 38% and 77% the volume of the engine. In their study, they saw an improvement of 7% in HC conversion efficiency when moving to the larger volume. This is similar to the improvement of 5% seen at 5 kW moving from one to two cartridges. Hsien states that "the converter size is suggested to be close to or more than the engine displacement." This statement aligns with what was observed in this testing. The three cartridges are equal to 115% of the engine volume and effectively convert emissions at all loads.

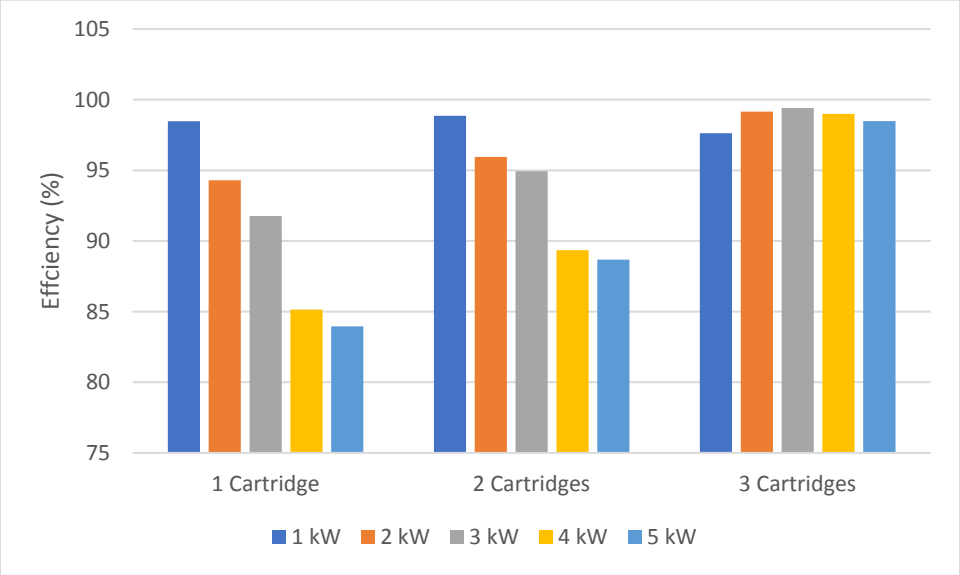

Figure 29. Single-cylinder catalyst efficiency with three volumes

Figure 30 presents the data for the multi-cylinder engine. The plot groups by cartridge volume and shows the two different speeds that each point was run. The power labels state equivalent to indicate that they are the same airflow as the equivalent power seen for the single-cylinder. The data show the same trend seen in the single-cylinder, which is a decreasing

efficiency with increased load and overall efficiency improvement with additional mass of catalyst. As noted above, the general rule-of-thumb for multi-cylinder engines is sizing a catalytic converter from 50-80% of the engine volume. This means that the maximum catalyst volume tested here is only 19% of the multi-cylinder engine's volume. Even with this large discrepancy, it seems that the two cartridge system mostly eliminates the sharp drop off at 5kW and is eliminated with three cartridges. For this system analysis, it is better to analyze the 1800 RPM for the multi-cylinder engine since the 900 RPM points are generally well below standard operating points for the engine. It would be closer to idle rather than a point at driving speed.

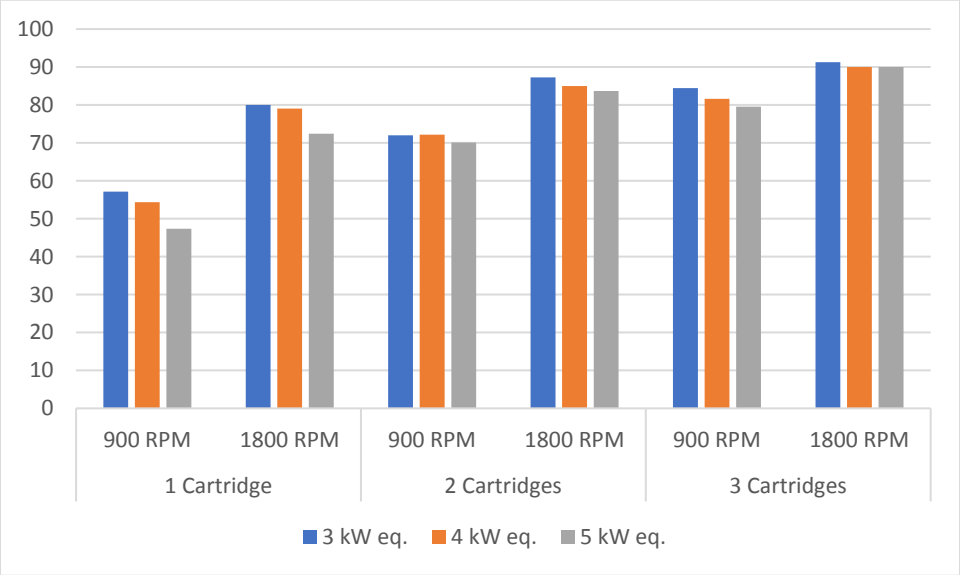

Figure 30. Multi-cylinder catalyst efficiency with three volumes and two engine speeds

Analyzing the impact of engine speed on efficiency, the 1800 RPM engine speeds exhibit higher efficiencies due to the smoothing of the airflow, increased temperature, and elimination of reverse flow (Figure 31). The single cartridge system saw improvements up to 25% with the increased pulsations. The exhaust pressure never drops below ambient pressure at the higher engine speeds as indicated by Figure 28. The reverse flow could be causing issues with extra oxygen diluting the exhaust and eliminating the benefit of a controlled oscillation around

stoichiometric for the fuel control system. Another issue that can be present with reverse flow is the induction of cooler air causing the catalyst to drop below its effective temperature (Liu, 2000).

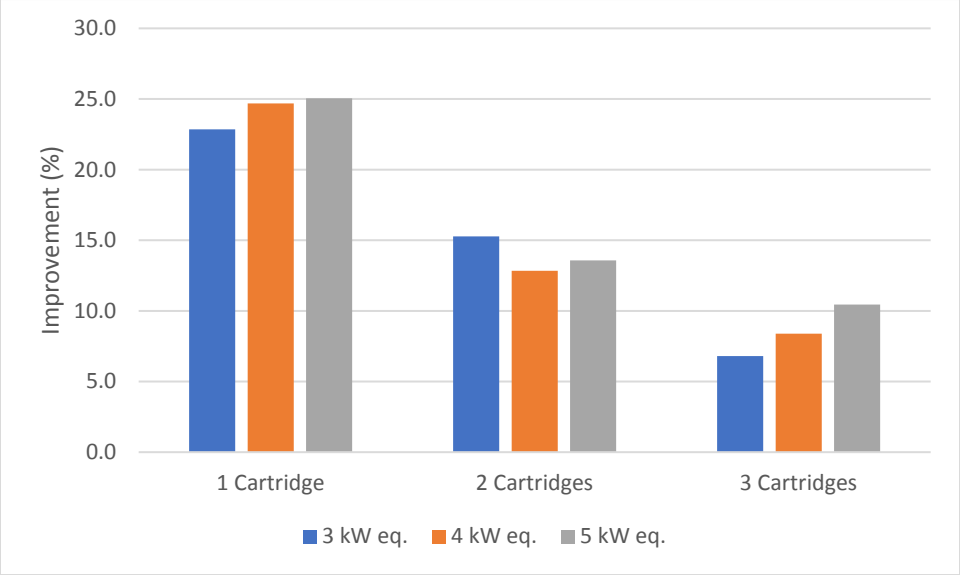

Figure 31. Percent points improvement by increased engine speed moving from 900 RPM to 1800 RPM

Comparing the single-cylinder and multi-cylinder with the same pulse frequency, it is seen that the average efficiency is lower on the multi-cylinder at a given load condition. As noted before, this is likely from the higher compression ratio, better combustion system, and total distance to the catalyst leading to lower catalyst temperatures. To compare the engines, the efficiency values from each engine were normalized. This was accomplished by assuming the efficiency would move proportionally with the temperature curve of the catalytic converter. Once they were normalized, then the points could be compared that were run on both engines. Figure 32 represents the difference from the efficiency achieved at the 3 kW point, and positive represents a decrease in efficiency from this point. The numbers are fairly similar and exhibit the

same trend, but the three cartridge point on the multi-cylinder decreases more than the single-cylinder.

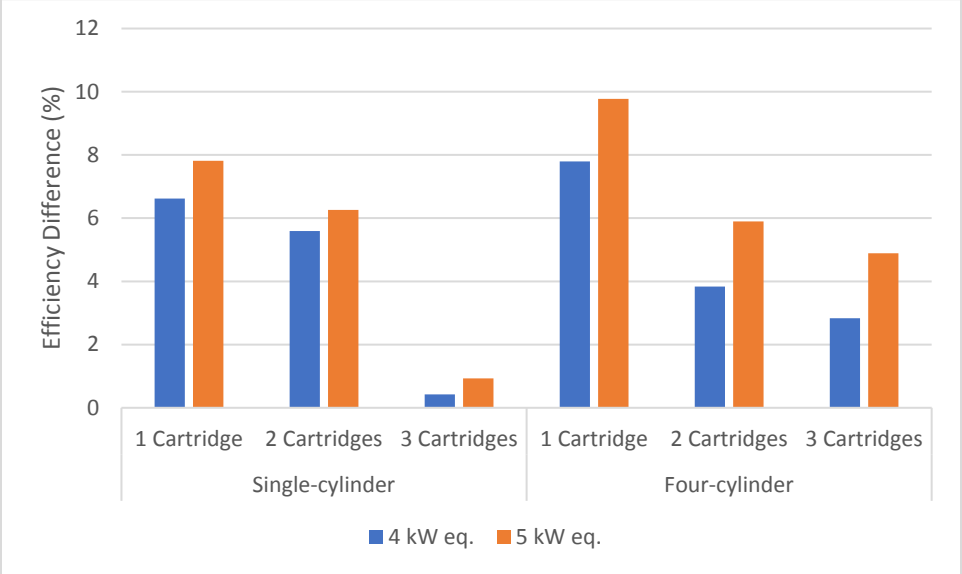

Figure 32. Normalized efficiency difference from 3 kW

Conclusion

A catalyst mass study was performed on two engines to determine the impact of pulsation and flow on the efficiency of a catalytic converter. Future standards will necessitate the use of catalytic converters and an understanding for small, single-cylinder engines needs to be understood. A custom catalyst housing was fabricated to hold catalyst cartridges to vary the mass of the catalyst. The housing was also designed to have ports throughout its length to measure emissions, temperature, and pressure data. The pressure data provided a view of the exhaust flow and difference of pulsation amplitude between engines and speeds.

A single-cylinder engine was run from no load up to peak load to determine the amount of catalyst to be effective at all loads. The airflow was then matched on a multi-cylinder engine to analyze the impact of pulsation on the efficacy of a given mass of catalyst. This was

accomplished by doubling the frequency by varying the engine speed. Future work can quantify the impacts of temperature, frequency, and pressure.

Significant highlights include:

- Catalyst efficiency dropped with increased load on both engines, indicating catalyst sizing was not adequate with low catalyst volume.
- Emissions efficiency became level at all loads for the single-cylinder engine at 115% catalyst volume compared to engine volume. The same efficacy was seen on the multi-cylinder engine with only 19% of the engine volume.
- Higher frequency of pulsations improves efficiency by reducing reverse flow through the catalytic converter. This reduced the amount of blow-by due to high velocity pulses, increased residence time, and also provide elevated temperatures. Low catalyst mass saw up to 25% improvement with higher pulsation frequencies on the multi-cylinder engine.

REDUCTION OF HEAT LOSS AND APPARENT POWER THROUGH GENERATOR FREQUENCY CONTROL

Overview

Generators, or gensets, pair an electric generator with an engine to be able to provide power in remote situations or in case of power loss. They are designed to be reliable and cheap, while also having very few regulations to dictate their performance. This leads to inefficiency across the board for the components.

General purpose utility engines are designed for a wide variety of applications. They range in power up to 19 kW, are intended for non-road use only, and are usually operated over a narrow speed range with varying loads. This works well for applications such as power generators, lawn mowers, or handheld lawn equipment.

Fixed speed operation is desirable for power generator applications since, for synchronous generators, the electrical power output frequency is directly proportional to the generator rotor rotational speed. Constant electrical power frequency is preferred, and even regulated for electric utilities because many loads are frequency sensitive. For inductive loads, frequency deviations result in impedance deviations and thus current magnitude changes. A decreasing frequency increases current magnitude and therefore increases the reactive power absorbed by the load. Such is true for both large stationary generators and small portable units powered by small engines. Small spark-ignited engines are good choices for such portable applications since they are lightweight and inexpensive relative to alternatives such as small diesel engines, gas turbines,

or fuel cells. Incorporating advanced technology into these engines, such as the control strategies described herein, enables them to operate with significantly higher efficiency and significantly lower emissions than they are historically known for producing.

Background

An AC synchronous generator is one in which the frequency of the output voltage and current is directly proportional to the rotor speed. The generator has windings on both the rotor and the stator. To establish the magnetic field in the air-gap of the generator, a winding on the rotor is excited with a dc current. The resulting rotating magnetic field induces a sinusoidal voltage on the stator winding which supplies the load. The dc rotor current controls the magnitude of the voltage induced on the stator. A simple voltage regulator on the rotor winding provides a cheap and robust solution for rotor current control.

The power output of the genset is proportional to the square of the magnetic flux produced on the rotor. The current that controls the rotor magnetic flux is determined by the onboard voltage regulator. The voltage regulator taps the outputs of the stator to measure the voltage output, rectifies the ac signal, and then scales the current necessary to achieve the desired output voltage. An example of a voltage regulator control scheme is shown in Figure 4.

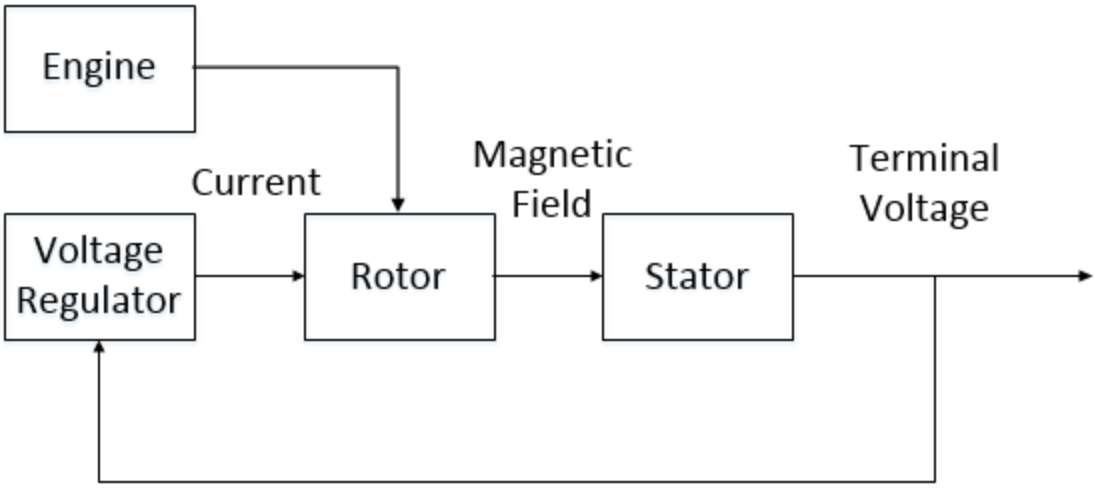

Figure 33. Simplified diagram for method of controlling voltage output of generator

As the load increases, the terminal voltage will sag due to the winding impedance. The voltage regulator will then increase the current on the rotor to boost the voltage back up to operating range. Another condition is when the frequency droops. The generator's reactive power output increases and the voltage regulator must also boost its current to make up for the resulting real power losses that occur with the increase in load current.

The voltage regulator does not affect the output frequency, so the frequency of the genset is directly defined by the engine speed. This means the output frequency droops under heavy loads due to the nature of the mechanical engine speed governor. More expensive generators will use multiple stators to allow for voltage control and also for reactive power reduction (Saptarshi Basak, 2017), but this is too expensive of a solution for low power applications.

Engine Controls. Traditional (low-technology level) small engines use entirely mechanically based systems for controlling speed, fuel, and spark. Many designs are simplified carryovers from vehicle systems from decades or even a century ago. Without the stringent emissions requirements like vehicles face, the small engines have been able to survive with the

mechanical solutions not requiring any further research or design. The following paragraphs discuss traditional engine speed, fuel, and spark

The traditional method of controlling speed is through a mechanical governor such as the centrifugal flyball governor shown in Figure 2. This device is based on the kinetic energy of weights spinning with a rotational velocity proportional to the engine's crankshaft. A linkage mechanism connects these weights to the engine's throttle. As their rotation speed increases, the weights move outward causing the throttle to close. This arrangement provides proportional engine speed control by balancing the torque produced by the engine with the applied load to the engine.

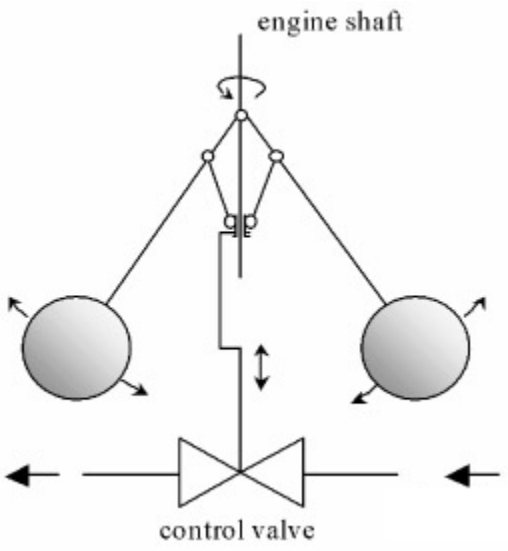

Figure 34. Control schematic for centrifugal governor (Spec, 2006)

Such a proportional system suffers from inherent speed droop with load. This is because more airflow is required in the engine to increase torque, and to provide the extra air needed to produce the torque, the throttle has to open more which only happens with reduced speed Figure 35. Increasing the proportional gain (the lever ratio between the balls and the throttle or reducing the spring stiffness (when present) that restrains the flyballs will reduce the droop but will

increase the tendency for the speed to overshoot its setpoint. To eliminate the droop and control the overshoot, integral and derivative effects must be incorporated into the mechanism.

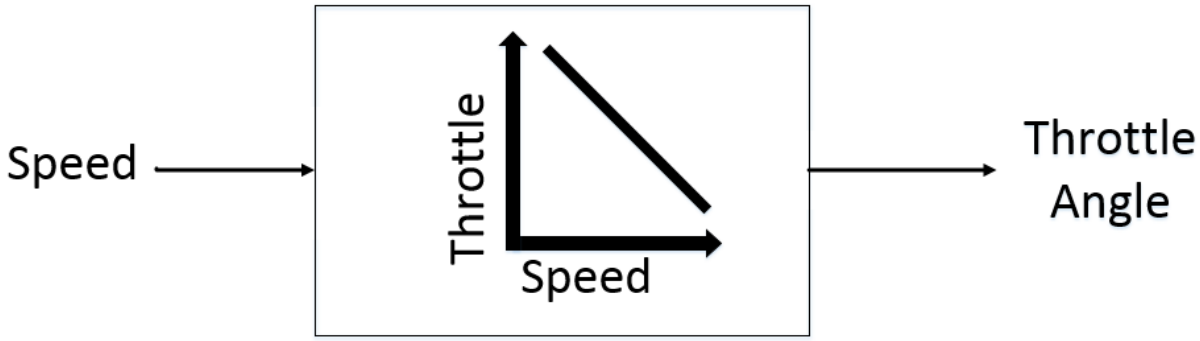

Figure 35. Flow Diagram Representing Control System for Mechanical Governor

The centrifugal governor only allows for proportional control because of its design. Mechanical solutions for the integral and even derivative terms have been designed, but are incredibly complicated and expensive. Figure 3 gives an example of a system that controls proportional, integral and derivative terms and shows the complex mechanical systems it requires.

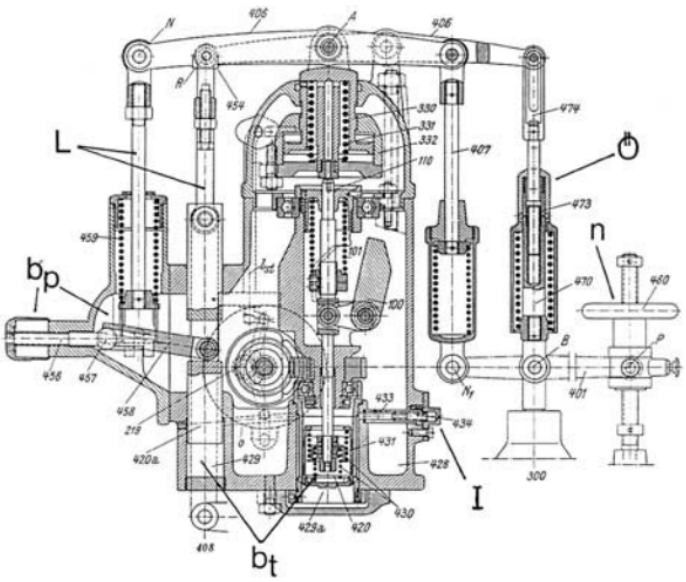

Figure 36. Mechanical governor with proportional, integral, and derivative capabilities (Springer, 1940)

An electronic throttle is the next generation for engine control and is used in almost every automotive application currently. It eliminates every downfall of a mechanical governor, but at a higher price. By being able to control throttle position with software, engine speed can remain constant at any desired speed. This prevents the droop in engine speed experienced by engines with mechanical governors.

The use of electronic throttle control has been researched for large engines using more complex control systems (Sehwa Choe, 2016), but not on smaller, personal-use generators. Alternative solutions exist to supplement power to reduce speed deviation, especially on load changes. These systems use supercapacitors and batteries to allow for a smoother transition and lower generator loads temporarily (Kosseila Bellache, 2018).

Types of Power. Most generators available for home use in the United States are designed to run at 3600 RPM to provide the 60 Hz frequency used for all AC powered devices. In power plants, very complicated and important control systems are in place to minimize any

frequency disturbance and to keep the long-term average at a very precise 60 Hz. The system is also helped by having many synchronous generators connected so that all are spinning at the same speed and resist any change (Mobarak, 2015). Some systems limit load to maintain a maximum rate-of-change on certain parameters to keep them within limits (Cruden, 2007). Although power plants are very resilient to load changes, even commercial power solutions such as wind turbines can experience power factors as low as0.5 during a load change (Md Moinul Islam, 2016).

Generators currently force consumers to accept the penalties for frequency deviation and hope no harm is done to the devices the generators power. This allows for cheap engines to be used to power the generator and have a wide speed range. Generators are generally set to run at 3600 RPM at no load which means that engine speed will only become lower at any speed, so the max frequency seen by any load will be 60 Hz.

Figure 5 shows the equivalent circuit for a typical generator. It has been simplified to contain a resistance (R_s) and reactance (X_s) to characterize the generator. The terminal voltage (V_t) represents the interface to the user loads, and the load is simply a resistance (R_L).

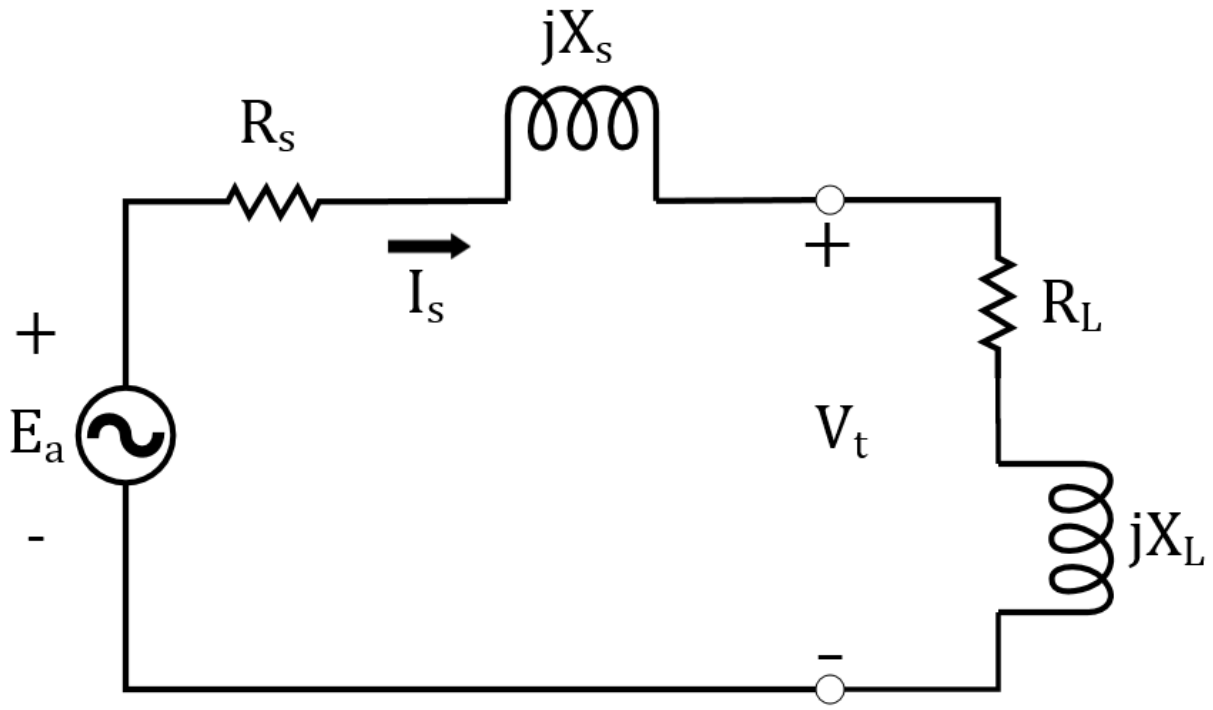

Figure 37. Schematic of generator with load

The frequency deviation has an effect of the apparent power produced by the generator. For a given load, the resistance and inductance will remain constant. Equation 21 shows how current for the system is calculated.

$$\bar{I}_s = \frac{V_t}{R_L + j\omega L_L} \tag{21}$$

Since voltage will remain controlled by the voltage regulator, and the resistance and inductance will both remain constant, the system current will increase due to the reactance from the inductive load decreasing. The increased current leads to higher losses due to heat generation in the windings from resistance as noted in Equation 22.

$$P_{loss} = \bar{I}_s^2 * R_s \quad (22)$$

The heat loss decreases the efficiency of the generator and proportionally increases the fuel required to produce a given generator load. The reactance also creates an undesirable type of power called reactive power which cannot be used by the load. By plotting complex power in the complex plane (Figure 6) where real power (P) is on the real axis, and reactive power (Q) is on the imaginary axis, the magnitude becomes known as apparent power (S).

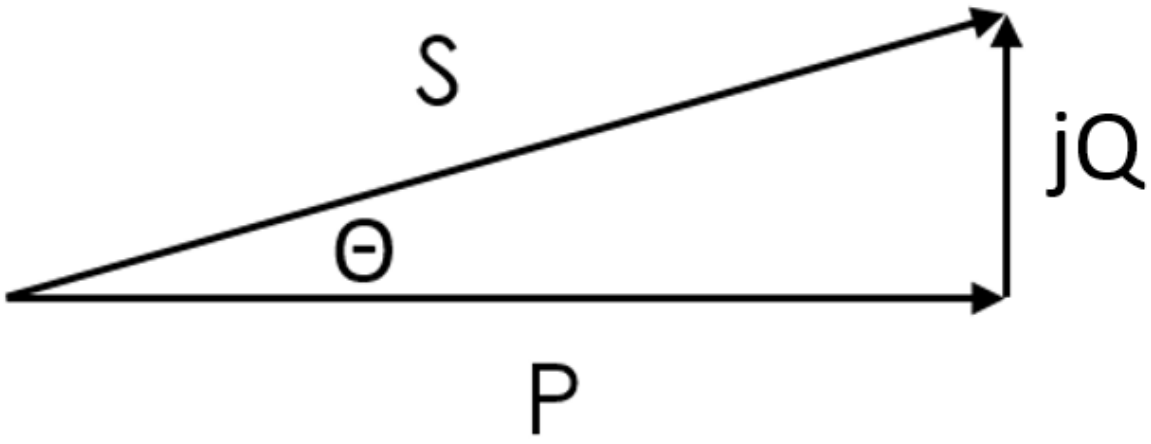

Figure 38. Power phasor diagram

So as reactive power increases, apparent power must also inherently increase. This increase in apparent power, especially at reduced power factors, leads to less real power being able to be delivered at peak load for a given diameter of motor winding wire. The engine operating at 60 Hz will reduce the reactive power at a given load and improve the efficiency of the overall system.

Test Setup

The genset used in this experiment Powermate 5500 generator, which is a common version available at many stores. It comes equipped with a Honda GX390 engine. It is a single-cylinder,

389cc displacement, air-cooled engine. It has been modified for other testing to have electronically controlled port fuel injection and electronic ignition.

The generator is a synchronous generator with a capability of providing 240 volts ac and 5500 VA continuously and 7000 VA at peak load. The windings have been center tapped to also provide 120 volts AC.

The ECU used is a cRIO from National Instruments with a Drivven package. Drivven is designed to allow for rapid-prototyping of engine control systems. The cRIO is responsible for all inputs and outputs to run the engine. The inputs are intake air temperature, manifold air pressure, throttle position sensor, and an oxygen sensor. The outputs are servo position to control the throttle, fuel injector pulsewidth for mass injected and timing based on crank angle, and a logic signal to control spark driver dwell time and also timing. The engine controller uses the speed-density (Reif, 2015) to control fuel. The MAP is read at the required engine crank angle to measure the lowest pressure in the system. This is done specifically and critically on single-cylinder engines due to the physics of the intake system. Since the intake is only being drawn on for about a quarter of the time, pressure is variant throughout the cycle. The intake system will be around atmospheric while the intake valve is closed and then drop to its lowest pressure somewhere around maximum piston velocity on the intake stroke. This minimum pressure location is empirically determined, and a calibration table is created with speed and load axes. This pressure is then combined with the air intake temperature in the ideal gas law to determine the mass of the air in the ideally full cylinder. Due to throttle losses and intake dynamics, the cylinder is not always full. This ratio of actual mass of air in the cylinder compared to the mass if it were completely full is known as volumetric efficiency and is empirically calibrated and input

into a table based on engine speed and MAP. This controller also controls the servo for the throttle to provide instantaneous control.

The method for speed control implemented on this test engine is an electronic throttle. It is controlled using a servo which allows precise control of the throttle angle and allows for a proportional/integral controller that can be calibrated when desired instead of inherently designed into the hardware. The system chosen to provide the electronic control is a servo directly connected to the throttle with a linkage and an encoder attached to the throttle to provide feedback. This system also provides for any speed control and fixes the issue of speed droop. The control system PI controller is shown in Figure 39.

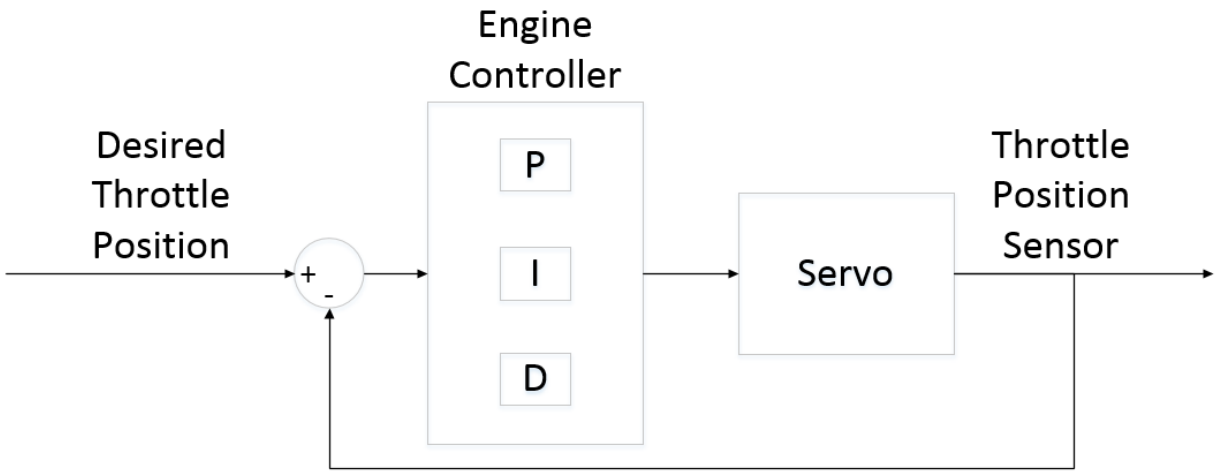

Figure 39. Flow diagram of control system for electronic throttle controller

Characterizing Generator

The generator was characterized using an equivalent series resistance and inductance, and the terminal voltage was measured at the output of the windings. Figure 5 shows the schematic for the system with an additional known load resistance. The generator (R_S) resistance was the most straightforward to measure since it was done with the system off and measured across the

terminal. This was measured with a GW Instek GOM-804 DC Milliohm meter with the 4-wire leads.

The next step was to determine the inductance of the generator. The inductance must be calculated at the rated speed for the system and thusly cannot be directly measured. To accomplish this, a resistive load bank was connected to the generator, and the current through it was measured as the field current through the stator was varied. This provided information on the method of control that the voltage regulator uses. The voltage and current from the output of the voltage regulator were recorded along with the terminal voltage for comparison. A Tektronix DPO4034 with a bandwidth of 350 MHz and a sampling rate of 2.5 GS/s was connected to the voltage regulator output and voltage terminal to measure the voltage and current simultaneously. The voltages were measured with diff probes to prevent any issues of a shared ground short-circuiting the system, and the currents were measured with Tektronix TCP0030A current clamps.

First, the system was run at no load and then at a high load to get the baseline measurements. The current was observed to increase as expected with the increased load to maintain the desired voltage. The voltage regulator was then removed and replaced with an external power supply to emulate the voltage regulator. The power supply was connected directly to the leads leading to the rotor to directly control the magnetic field. An equivalent current was supplied with no load on the system, and the terminal voltage achieved the desired voltage. The current was then left the same, and the load was increased. The terminal voltage then droops to almost half of the desired voltage. These values can be seen in Table 8.

	Terminal Voltage (V)	Terminal Current (A)	Field Brush Voltage (V)	Field Brush Current (A)
No load - Stock Regulator	239.2	0	80	0.7
4 kW - Stock Regulator	238.6	16.6	114.5	1.2
No Load - Power Supply	239.5	0	43.1	0.7
4 kW - Power Supply	143.4	10.35	29.7	0.6

Table 8. Summary of Field Brush Measurements

The following calculations show the method for determining the generator inductance. They are calculated using the 4 kW external power supply data. This provides a point at which the field voltage (E_A) is known.

The 4 kW load used in the measurements provides a resistance of 14.4 Ω which was verified as seen below.

$$R_L = \frac{V_T^2}{P} = 14.4\ \Omega \tag{23}$$

The current of the system was then calculated using the measured terminal voltage and the calculated resistance.

$$\bar{I}_s = \frac{V_t}{R_L} = 9.96\ A \tag{24}$$

The system current, field voltage, load resistance, and generator resistance are all known at this point. The final load to determine was the reactance (X_S) due to the inductance of the generator.

$$\bar{I}_s = \frac{E_a}{\sqrt{(R_L + R_S)^2 + X_S^2}} \tag{25}$$

Knowing the reactance, the inductance can finally be calculated. It turns out to be a very neat 50 mH.

$$X_S = \omega L_S = 18.85\ \Omega \Rightarrow L_s = 50\ mH \tag{26}$$

System Model

The system can be modeled knowing the system resistance, inductance, and that the terminal voltage remains constant. The model will simulate from no load up to the peak power of 7 kW

and will run through different power factors. The power factor range has been decided to be .7 – 1 by looking at those of typical devices that can be seen in Table 9.

Appliance	Power Factor
Induction Motor - Loaded at 0%	0.17
Induction Motor - Loaded at 50%	0.73
Induction Motor - Loaded at 100%	0.85
Incandescent Light	1
Fluorescent Light (uncompensated)	0.5
Fluorescent Light (compensated)	0.93

Table 9. Power Factors of Typical Appliances (Schneider, 1996)

The model will be designed to compare and show the benefits of using an electronic throttle to maintain engine speed at the desired speed. It will achieve this by determining the load characteristics, resistance, and inductance, of the various loads. It will then hold these characteristics constant as it varies the frequency of the system that they experience. The two speeds that will be simulated are 60 Hz as the desirable speed seen by the electronic throttle system and a lower speed that can be empirically determined from engine data based on load. These two points will have the current and apparent power solved and compared. The current difference will determine the efficiency improvement seen due to heat loss from the resistance and the fuel improvement gain for the engine. The apparent power difference will indicate the reduction in generator size that is possible. Models based on apparent power have also been used

to create “Stalling Zone” maps to prevent the throttle controller from moving into those areas (Abrez Mondal, 2014).

The model steps through the full range of complex loads the genset is capable of running and range of typical power factors. It is a two-step process that first calculates the values for the mechanical governor system and then determines the difference for the electrical governor system with an assumed constant speed of 3600 RPM. At each point, the angle of the lagging current is found based on the given power factor.

$$\Theta = \cos^{-1}(PF) \tag{27}$$

Based on the calculated angle, the real and reactive power are found.

$$Q = S * \sin(\Theta) \tag{28}$$

$$P = S * \cos(\Theta) \tag{29}$$

The complex load is found at each breakpoint for the mechanical system by dividing the terminal voltage by the complex power vector.

$$\bar{Z}_L = \frac{V_t^2}{\bar{S}_L} \tag{30}$$

The complex load impedance is then broken into its constituents of resistance and reactance.

$$\bar{Z}_L = R_L + jX_L \tag{31}$$

The inductance for each load is then calculated based on the mechanical speed. This becomes the point of comparison for the entire model as the inductance and resistance will remain the same for every breakpoint, but the complex load for the electrical governor system will be different due to the higher frequency.

$$L_L = \frac{X_L}{\omega} \tag{32}$$

The resistance and inductance are then used to determine the complex load for both the mechanical throttle system (drooped speed) and electrical throttle system (constant 60 Hz). The current for both systems is found based on their respective load impedances.

$$\bar{I}_s = \frac{V_t}{\bar{Z}_L} \tag{33}$$

The current is finally used in the power loss equation to determine how much power is lost to heat due to the resistance of the windings. This loss can be compared against the real power output of the generator to see its impact on the load the engine sees. I_S

$$P_{loss} = \bar{I}_S^2 * R_S \tag{34}$$

The apparent power for both systems is also calculated. This determines how much the generator efficiency will improve for flowing a unit of real power compared to the total apparent power. The entire model has been simplified in Figure 40. The model splits into calculating the mechanical throttle system and electronic throttle system after determining the complex load for each power factor. The load resistances (R_L) will be the same for both systems, but the load reactance (X_L) will differ due to the frequency difference.

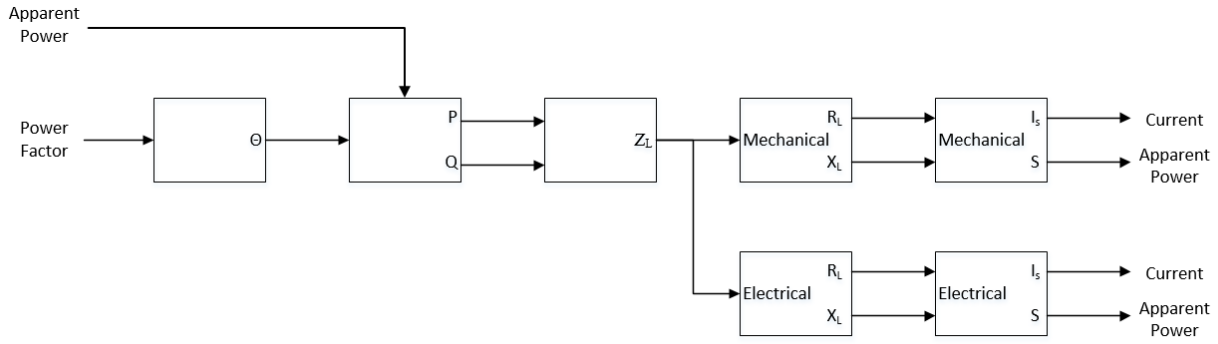

Figure 40. Flow diagram for model used to determine system values

Results

The following plots all come from the Matlab model for the generator. In each plot, each line indicates a different power factor and the plots indicate the difference between the mechanical throttle (frequency droop) and the electrical throttle (constant 60 Hz). Since improvements will range between zero and maximum at the worst-load, only the worst-load will be discussed.

The first comparison is looking at benefits within the generator. The system will generate heat with current, so reducing any unnecessary current will also reduce the heat generated. Heat generation in the windings is reduced by over 12.5% compared to the baseline heat loss at peak load as seen in Figure 41. This improvement varies linearly with load with the greatest benefit at the highest load.

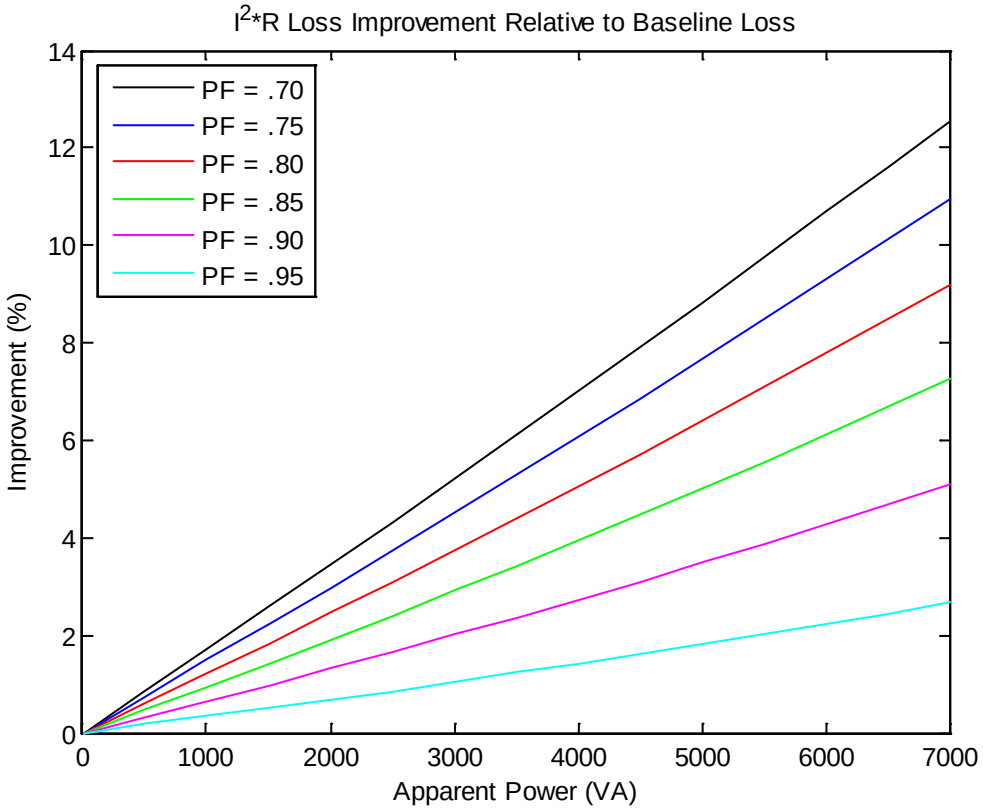

Figure 41. Improvement in Heat Loss Due to Current in Generator Windings

This equates to a reduction in total power consumption of about .8% in relation to the total real power output. Since the only load the engines sees is the real power, this reduction in heat loss equates to the same amount of reduction in fuel flow. A .8% reduction in fuel consumption for any engine is considered good especially since millions of engines are purchased. Even at better power factors, the gain is significant.

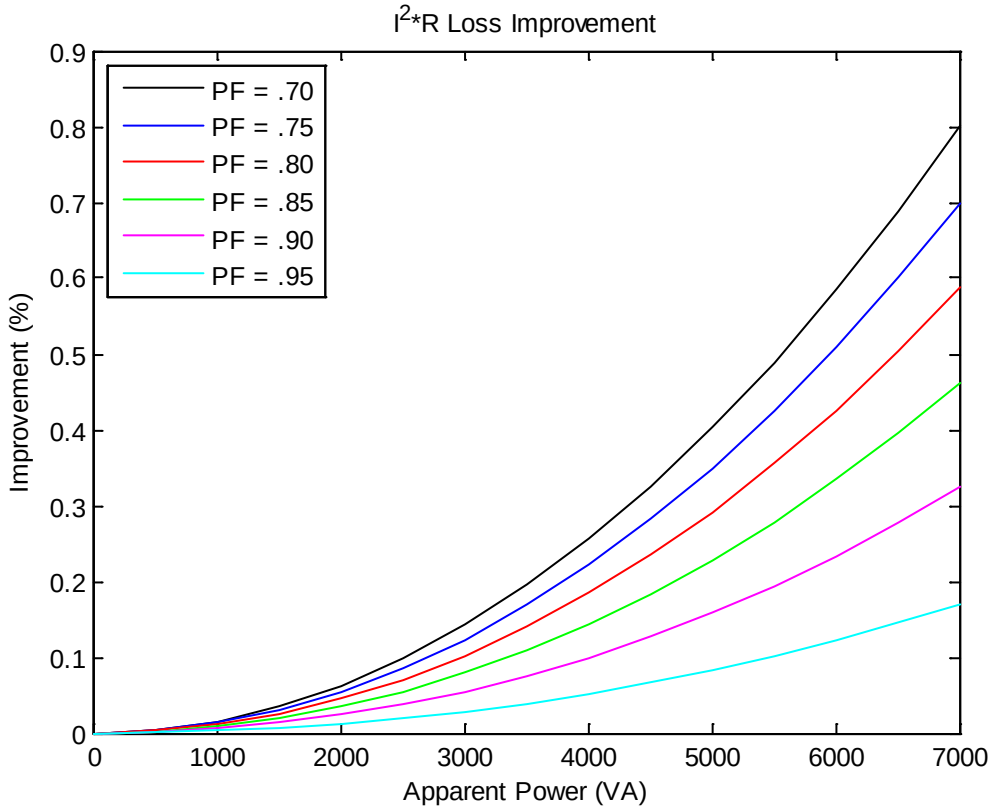

Figure 42. Heat Reduction Compared to Total Real Power

The most significant improvement is seen in the apparent power reduction. Over 450 VA less apparent power is generated for the equivalent real power load. This is an improvement of

6.5% and can be seen in Figure 43. Apparent power requires the copper winding gauge to be increased, so being able to reduce the gauge and thus mass of copper required is very desirable.

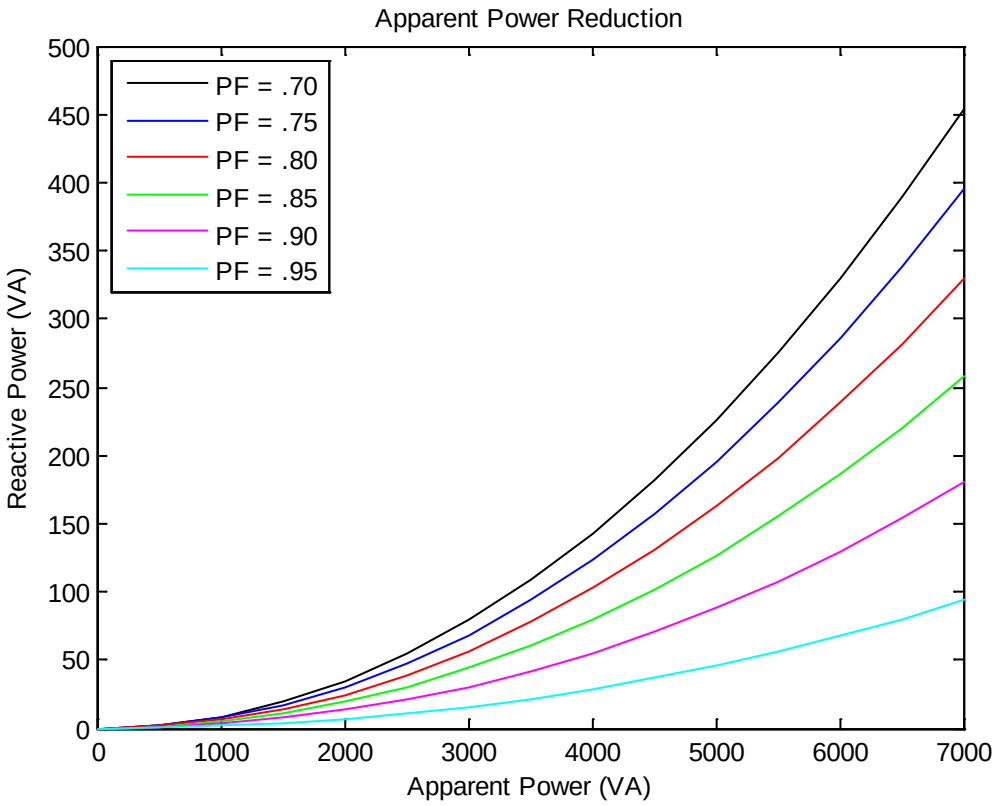

Figure 43. The Reduction of Apparent Power Compared to Load

These combined results to the system show a very significant improvement over the baseline system. Less fuel flow and generator capacity are needed to be designed to meet the desired specifications.

Conclusion

A genset with a general-purpose engine and synchronous generator was updated with an electronic throttle to determine the benefits of the system. The electronic throttle would eliminate the speed droop, and thus electrical frequency droop, that a flyball governor causes. Reactive

power increases as electrical frequency drops below 60 Hz, so the overall apparent power will decrease by maintaining engine speed. This will, in turn, improve the efficiency of the generator through reduced heat loss and less system current requirements.

The synchronous generator was characterized by resistance measurements and inductance measurements while running. The mechanical governor on currents engines causes speed droop at any load, so the speed slope was determined. The generator had the voltage regulator and terminal voltage measured at various operating points to determine its operation. The entire system was then modeled to determine the benefits that would be seen by implementing an electronic throttle and thus a fixed frequency at 60 Hz. At the worst-load situation, the best results are seen as summarized:

Significant highlights include:

- The reduced current seen at low power factors and high load reduced the heat generated in the windings of the generator by 12.5% over the baseline heat loss
- This reduced heat loss means up to .8% in fuel reduction for the engine as the only load the engine sees is the real power generated by the generator, which the heat loss is included in.
- The constant speed reduced the reactive power leading to the apparent power dropping by 6.5% reducing the design need for copper material in the windings since less system current capacity is required.

CONCLUSION AND RECOMMENDATIONS

Three methods were investigated to improve the efficiency and reduce the emissions of a small portable gasoline power generator using a combination of advanced controls and hardware. This chapter summarizes the conclusions from the three independent efforts to achieve this goal. This work was an extension of a major effort funded and led by the US Consumer Product Safety Commission to reduce CO emission poisoning from these portable generators. While the CO poisoning considerations consider the emission problem from a different perspective than that held by the Environmental Protection Agency, who is tasked with maintaining healthy atmospheric air quality and not necessarily as concerned with close quarters effects of small engine emissions, arguments made in the introduction to this work show that emission standards for small non-road engines are too lenient and should be tightened. The three independent efforts alluded to above included implementing electronic engine controls and developing a novel predictive flow algorithm to improve fuel control during transient operation, studying catalytic converter sizing requirements for single-cylinder engines and comparing those requirements to those associated with multi-cylinder engines, and finally investigating the impact of engine speed control on the alternator performance. The conclusion summary is followed by recommendations for future research.

Effort One: Predictive Fueling Algorithm using Electronic Throttle Actuation. The benefits of applying modern electronic engine control to the engine powering a small portable generator were investigated. The electronic system included an electronic throttle actuation which had the primary benefit of eliminating the load-induced speed droop associated with

mechanical flyball type governors but also facilitated the possibility of implementing a simultaneous air and fuel control strategy that could potentially reduce emissions during transient operation. The throttle was modeled using a flow bench to determine its flow characteristics as functions of throttle blade angle. These data were incorporated into a simple pseudo-steady flow model of the throttle restriction. This model was used to augment the fuel injection duration to account for the anticipated air flow for the next engine cycle.

Engine dynamometer tests were run based on real-world cycles to evaluate the impact of electronic engine control and the advanced predictive fuel control algorithm for the consumer portable generator market. The results of this study show that electronic throttle control and the advanced algorithm led to significant respective improvements in speed control and transient fueling accuracy which resulted in reduced emissions. Future work can further reduce emissions with smarter closed-loop fueling management, using throttle acceleration rates to determine a more accurate future throttle position, and using a better model to predict MAP.

Significant highlights include:

- Closing the loop on the electronic fuel control using an exhaust oxygen sensor decreased equivalence ratio deviations from stoichiometric by 33% and reduced HC emissions by 20% over the multi-load test cycle.
- Incorporation of the electronic throttle with proportional-integral control virtually eliminates the speed droop associated with simple proportional flyball governors typically installed in this market. The generator unit tested exhibited more than 300 RPM of droop at the maximum 5 KW load compared to the no-load condition with the OEM mechanical governor. While the steady-state droop was eliminated with the electronic throttle, the settling time took as long as ten seconds in the most extreme

load transitions, whereas it was nearly instantaneous with the mechanical throttle. It is likely further tuning of the PID parameters or implementation of a more robust throttle control algorithm could reduce or eliminate this discrepancy, but this was not pursued as part of this work.

- Finally, using the fully electronic system (fuel and throttle) the predictive fuel control algorithm improved 66.7% compared to the results using a conventional control strategy. The emission improvement represents a 34% reduction from the baseline open-loop electronic setup. It is worth noting the baseline setup is already a large improvement over the carbureted fueling typical of small engines being sold today.
- The gains from the predictive algorithm were achieved without any additional engine calibration beyond what was performed for the closed-loop strategy without predictive control strategy. The only additional work required for incorporating the algorithm was to characterize the throttle flow.

Effort Two: Single-Cylinder Catalyst Study. A catalyst mass study was performed on two engines to determine the impact of pulsation and flow on the efficiency of a catalytic converter. Future standards will necessitate the use of catalytic converters and an understanding for small, single-cylinder engines needs to be understood. A custom catalyst housing was fabricated to hold catalyst cartridges to vary the mass of the catalyst. The housing was also designed to have ports throughout its length to measure emissions, temperature, and pressure data. The pressure data provided a view of the exhaust flow and difference of pulsation amplitude between engines and speeds.

A single-cylinder engine was run from no load up to peak load to determine the amount of catalyst to be effective at all loads. The airflow was then matched on a multi-cylinder engine

to analyze the impact of pulsation on the efficacy of a given mass of catalyst. This was accomplished by doubling the frequency by varying the engine speed. Future work can quantify the impacts of temperature, frequency, and pressure.

Significant highlights include:

- Catalyst efficiency dropped with increased load on both engines, indicating catalyst sizing was not adequate with low catalyst volume.
- Emissions efficiency became level at all loads for the single-cylinder engine at 115% catalyst volume compared to engine volume. The same efficacy was seen on the multi-cylinder engine with only 19% of the engine volume.
- Higher frequency of pulsations improves efficiency by reducing reverse flow through the catalytic converter. This reduced the amount of blow-by due to high velocity pulses, increased residence time, and also provide elevated temperatures. Low catalyst mass saw up to 25% improvement with higher pulsation frequencies on the multi-cylinder engine.

Effort Three: Impact of Electrical Frequency on Generator Efficiency. A genset with a general-purpose engine and synchronous generator was updated with an electronic throttle to determine the benefits of the system. The electronic throttle would eliminate the speed droop, and thus electrical frequency droop, that a flyball governor causes. Reactive power increases as electrical frequency drops below 60 Hz, so the overall apparent power will decrease by maintaining engine speed. This will, in turn, improve the efficiency of the generator through reduced heat loss and less system current requirements.

The synchronous generator was characterized by resistance measurements and inductance measurements while running. The mechanical governor on currents engines causes speed droop

at any load, so the speed slope was determined. The generator had the voltage regulator and terminal voltage measured at various operating points to determine its operation. The entire system was then modeled to determine the benefits that would be seen by implementing an electronic throttle and thus a fixed frequency at 60 Hz. At the worst-load situation, the best results are seen as summarized:

Significant highlights include:

- The reduced current seen at low power factors and high load reduced the heat generated in the windings of the generator by 12.5% over the baseline heat loss
- This reduced heat loss means up to .8% in fuel reduction for the engine as the only load the engine sees is the real power generated by the generator, which the heat loss is included in.
- The constant speed reduced the reactive power leading to the apparent power dropping by 6.5% reducing the design need for copper material in the windings since less system current capacity is required.

Recommendations

The predictive flow algorithm could be improved through characterizing the throttle angle response to the servo control. By using acceleration rates of the throttle angle, the predicted throttle angle would be more accurate leading to even less fueling error. The algorithm could also include a compressible flow model to increase performance at low throttle angles. The addition of measuring the rest of the typical engine-out emissions, such as NOx, CO, CO_2, and O_2, would provide a much broader view of the physics taking place for both the predictive flow algorithm and the catalyst study.

The catalyst study could also be improved by installing the catalytic converter for the multi-cylinder engine in a way that allows for temperatures to be matched between engines. This would eliminate the concern of efficiency being lower and allow a direct comparison for the exhaust pulsation frequency. A higher volume catalyst for the multi-cylinder would allow for comparable volumetric percentages of the engine displacement between engines to be analyzed and correlated.

The model used to simulate the alternator was fairly simplified and could have additional characterizations and effect modeled. Much of the model considered the schematic to be ideal, where real-world limitations could be added. These variables could include the air gap and rotor design and would allow for a more representative model to be simulated. This model could then be compared to real-world data by running the engine at equivalent load points.

REFERENCES

Abrez Mondal, D. K. (2014). Modeling, Analysis and Evaluation of Smart Load Functionality in the CERTS Microgrid.

Buyer, J. (2012). *TECHNOLOGY DEMONSTRATION OF A PROTOTYPE LOW CARBON MONOXIDE EMISSION PORTABLE GENERATOR* . Consumer Product Safety Commission.

CARB. (2017). Retrieved from https://ww2.arb.ca.gov/resources/fact-sheets/small-engines-california

Chapman, S. J. (1999). *Electric Machinery Fundamentals.*

Cheng, J. S. (2000). Throttle Movement Rate Effects on Transient Fuel Compensation in a Port-Fuel-Injected SI Engine. *International Spring Fuels & Lubricants*.

Collings, N. (1988). A New Technique for Measuring HC Concentration in Real Time, in a Running Engine. *SAE Technical Paper*.

CPSC. (2006). *Carbon-Monoxide-Questions-and-Answers*. Retrieved from https://cpsc.gov/Safety-Education/Safety-Education-Centers/Carbon-Monoxide-Information-Center/Carbon-Monoxide-Questions-and-Answers

Cruden, G. Q.-V. (2007). Development of a Small-Scale Generator Set Model for Local Network Voltage and Frequency Stability Analysis. *IEEE TRANSACTIONS ON ENERGY CONVERSION*.

EPA. (2016). *Timeline of Major Accomplishments in Transportation, Air Pollution, and Climate Change*. Retrieved from https://www.epa.gov/transportation-air-pollution-and-climate-change/timeline-major-accomplishments-transportation-air

EPA. (2017). *Transportation, Air Pollution, and Climate Change*. Retrieved from . http://www3.epa.gov/otaq/certdata.htm#smallsi

Farrauto, R. H. (2002). *Catalytic Air Pollution Control.*

Ganoung, D. (1990). Fuel Economy and Drive-by-Wire Control. *International Congress and Exposition*.

Haskew, T., & Puzinauskas, P. (2013). *Advanced Algorithm Development and Implementation of Enclosed Operation Detection and Shutoff for Portable Gasoline-Powered Generators.*

Haskew, Timothy Austin (Northport, A. P., Paulius V. (Tuscaloosa, A. S., Joshua (Madison, A. G., & Andrew (Tuscaloosa, A. (2018). *US Patent No. 9,880,973.*

Heywood, J. (1988). *Internal Combustion Engine Fundamentals.*

Kohler. (2019). *Command Pro EFI ECH440*. Retrieved from https://kohlerpower.com/en/engines/product/command-pro-efi-ech440

Kosseila Bellache, M. B. (2018). Transient Power Control for Diesel-Generator Assistance in Electric Boat Applications Using Supercapacitors and Batteries. *IEEE JOURNAL OF EMERGING AND SELECTED TOPICS IN POWER ELECTRONICS*.

Liu, B. C. (2000). Experimental and Modelling Study of Variable Cycle Time for a Reversing Flow Catalytic Converter for Natural Gas/Diesel Dual Fuel Engines. *SAE Technical Paper*.

Md Moinul Islam, M. R. (2016). Analysis of Real-World Power Quality Disturbances Employing Time-Frequency Distribution.

Mobarak, Y. (2015). Effects of the Droop Speed Governor and Automatic Generation ControlAGC on Generator Load Sharing of Power System. *International Journal of Applied Power Engineering*.

OPEI, O. P. (2017). *Small Engine Fact Sheet*. Retrieved from opei.org/opei-small-engine-fact-sheet/

Pan-Hsiang Hsien, L.-K. H. (1992). Emission Reduction by Retrofitting a 125c.c. Two-Stroke Motorcycle with Catalytic Converter. *International Fuels and Lubricants Meeting and Exposition*.

Piero Azzoni, G. M. (1999). Air-Fuel Ratio Control for a High Performance Engine using Throttle Angle Information. *International Congress and Exposition*.

Prince, S. P. (1998). DRIVE BY WIRE ENGINE CONTROL USING AIR MODULATION. *Future Transportation Technology*.

Reif, K. (2015). *Gasoline Engine Management: Systems and Components.*

Saptarshi Basak, C. C. (2017). A New Optimal Current Control Technique for Dual Stator Winding Induction Generator. *IEEE JOURNAL OF EMERGING AND SELECTED TOPICS IN POWER ELECTRONICS*.

Schneider, G. (1996). *Electrical installation guide.*

Sehwa Choe, Y.-K. S.-K. (2016). Control and Analysis of Engine Governor for Improved Stability of DC Microgrid Against Load Disturbance. *IEEE JOURNAL OF EMERGING AND SELECTED TOPICS IN POWER ELECTRONICS*.

Shugang Jiang, M. H. (2009). Optimization of PID Control for Engine Electronic Throttle System Using Iterative Feedback Tuning.

Shun-ichi Akama, Y. M. (2013). Reduced-Order Modeling of Intake Air Dynamics in Single-Cylinder Four-Stroke Engine. *SAE Int. J. Engines*.

Spec, G. (2006). Retrieved from https://www.globalspec.com/reference/62558/203279/chapter-11-application-of-transform-techniques-to-lti-feedback-control-systems

Springer, J. (1940).

Takashi Takeuchi, H. T. (1983). Oxygen Sensors A/F Control.

Tessho Yamada, N. H. (1992). Universal Air-Fuel Ratio Heated Exhaust Gas Oxygen Sensor and Further Applications.

Transport Policy. (2018). *EU: Motorcycles: Emissions*. Retrieved from https://www.transportpolicy.net/standard/eu-motorcycles-emissions/

Woody, J. C. (1975). Small Engine Carburetors - State-of-the-Art.